STABILIZING HIGH EXPANSION FOAM USING ZIRCONIUM PHOSPHATE

A Thesis

by

ANAS AL-RABBAT

Submitted to the Office of Graduate and Professional Studies of
Texas A&M University
in partial fulfillment of the requirements for the degree of

MASTER OF SCIENCE

Chair of Committee,	Zhengdong Cheng
Committee Members,	Mustafa Akbulut
	Mahboobul Mannan
Head of Department,	M. Nazmul Karim

May 2018

Major Subject: Safety Engineering

ABSTRACT

Natural gas has been a fast developing industry for its advantages over other energy sources such as coal. Natural gas is usually stored as Liquefied Natural Gas (LNG). In the case of a leak of LNG, a potential risk for a fire hazard, a cryogenic vapor cloud, that is at a higher density than air, forms that travels downwind near ground level and could ignite upon contact with an ignition source. As a recommendation from The National Fire Protection Agency (NFPA) as well as the American Gas Association (AGA), high expansion foam is used to diminish the risk due to this vapor cloud by forming a "blanket" over the leaked LNG. This project intends to study the role of Zirconium Phosphate (ZrP) nanoplates in stabilizing high expansion foam. Experiments were performed with and without ZrP nanoplates to investigate nanoplate stabilization effects on foam stability. Experiments were also carried out in the presence of a cryogenic liquid (Liquid Nitrogen) spill along with the ZrP stabilized foam to examine ZrP effectiveness in mitigating the LNG vapor risk. Forced convection and thermal radiation were found to have significant effects on foam breakage. Adding the ZrP greatly enhanced the foams stabilization effect in reducing the foam breakage rate under forced convection and radiation. On the other hand, ZrP nanoplates have also reduced the liquid drainage rate under forced convection and thermal radiation which would, in turn, allow for extended time to transfer heat from the foam to as they make their way upwards through the foam layers; hence, a lower boil-off effect reducing the fire hazard of the leaked LNG.

DEDICATION

To my beloved family.

ACKNOWLEDGEMENTS

I would like to thank my committee chair, Dr. Zhengdong Cheng along with my committee members, Dr. Sam Mannan, and Dr. Mustafa Akbulut, for their guidance and support throughout the course of this research.

Thanks also go to my friends and colleagues and the department faculty and staff for making my time at Texas A&M University a great experience.

Finally, thanks to my mother and father for their encouragement, patience, and love.

NOMENCLATURE

LNG	Liquified Natural Gas
HEX	High Expansion Foam
LN2	Liquid Nitrogen
ZrP	Zirconium Phosphate
SEM	Scanning Electron Microscopy
TEM	Transmission Electron Microscopy
TBA	tetrabutylammonium hydroxide

CONTRIBUTORS AND FUNDING SOURCES

Contributors:

Part 1, faculty committee recognition

This work was suprtvised by a thesis committee consisting of Professor Zhengdong Cheng and Professor Mustafa Akbulut of the Department of Chemical Engineering and Professor Mahboobul Mannan of the Department of Safety Engineering.

Part 2, student contributions

All work for the thesis was completed by the student, in collaboration with Pratik Krishnan of the Department of Chemical Engineering.

Funding Sources

This work was made possible in part by the Mary Kay O'Connor Process Safety Center.

TABLE OF CONTENTS

Page

LIST OF FIGURES

Page

LIST OF TABLES

Page

CHAPTER I

INTRODUCTION/MOTIVATION FOR EXPANSION FOAM TO MITIGATE LNG LEAKAGE

1.1 LNG and LNG hazards

Natural gas consumption is expected to increase by nearly 70 percent over the next few decades as it is a cleaner source of energy compared to oil or coal and produces lesser amounts of carbon dioxide, sulfur oxide and nitrogen oxide per unit of energy produced.[1,2] In addition, advances in technology have enabled its extraction from sources previously considered to be economically infeasible. Liquefaction of natural gas can be an effective way of storing and transporting it because its volume is nearly 600 times lower in its liquid form and its exports are expected to increase.[2,3] A leak of liquefied natural gas (LNG) can result in the formation of a vapor cloud which can migrate downwind near ground level, exhibiting dense gas behavior as the density of methane is higher than air at low temperatures. This vapor cloud presents the danger of asphyxiation to any population in its vicinity and also has the potential to ignite. There have been several documented instances of LNG related incidents which have been summarized in table 1.[4,5,6,7]

An incident in 2004 at an LNG facility in Skikda, Algeria claimed 27 lives and resulted in over 70 injuries.[8] Another incident occurred in Plymouth, Washington, in 2014, in which an LNG tank was pierced by debris and resulted in an LNG leak and injured 5 workers. [9]

Table 1 : List of some LNG related incidents and their consequences

Ship / Facility Name	**Location**	**Year**	**Affect on human life**
East Ohio Gas LNG Tank	Cleveland, OH	1944	128-133 deaths
LNG Import Facility	Canvey Island, UK	1965	1 person burned
LNG export facility	Arzew, Algeria	1977	1 worker frozen to death
Columbia Gas LNG	Cove Point, MD	1979	1 killed, 1 injured
LNG export facility	Bontang, Indonesia	1983	3 workers died
Skikda I	Algeria	2004	27 killed, 72-74 injured
Atlantic LNG (Train 2)	Port Fortin, Trinidad	2006	1 person injured
LNG Facility	Plymouth, WA	2014	5 workers injured

LNG storage capacities have also increased since the past, for example LNG ship carrier's average size is around 120,000 m^3 whereas the ship carrier sizes currently in the production process are just under 160,000 m^3 and this is projected to increase further in the close future.[10]

1.2 High Expansion Foam application in mitigating LNG spills

The NFPA suggests the use of high expansion foam to mitigate the vapor risk of an LNG spill, (NFPA 11). This high expansion foam forms a vapor barrier containing the hazardous cryogen. In case there is a fire, the bubbles will help suffocate the flames and will help prevent re-ignition. [11]They are also gaining more attention as they tend to be biodegradable, making them environmentally friendly. [12] Just like water curtains in the

industry, the high expansion foam is applied as a mitigating factor to contain and prevent the re-ignition of the hazardous vapors.[13]

Foam is considered a metastable system (the bubble size gets larger as a function of time) as they display both solid and liquid like behavior. Foam is well known for its low density and large surface area because they contain a higher proportion of air.[14] Several factors exist that affect the stability of the foam such as the gravity segregation[15] drainage and coarsening of the foam. Gravity segregation is when liquid in the bubbles will be pulled towards the ground due to the effect of gravity. Drainage occurs when the liquid film in between the foam bubbles burst and causes the two bubbles to merge. Coarsening is the act of gas diffusing to a larger bubble due to the presence of a higher Laplace pressure in the smaller bubble.[16] Foams have a variety of uses such as in the food industry[17], firefighting[18], cosmetics[19,20], enhanced oil recovery[21], and other customer products.

There are several heat transfer mechanisms that can affect the vaporization rate of LNG in the presence of foam.[22] The foam blocks the effect of both convection and thermal radiation on LNG vaporization and is called as the blocking effect of foam. Liquid from the foam can drain over time and can increase the rate of vaporization of LNG. This is termed as the boil-off effect of foam. Over time, an ice layer forms since the temperature of the cryogenic liquid is far lower than the freezing point of water. This acts as a physical

barrier preventing direct contact of foam with LNG. However, as this ice is porous, it allows vapor to pass through. The blocking effect and boil-off effect are clubbed together and termed as the blanketing effect of foam and this highlights the net effect of foam addition and determines the vaporization rate of LNG. The vapors that pass through the foam layers exchange heat with the foam as they pass through, increasing their temperature. This increases the density of vapors making them more buoyant, which makes their dispersion easier. This is termed as the warming effect of foam.

While foam can block convection and thermal radiation, these heat transfer mechanisms can ameliorate foam breakage, altering the amount of foam that needs to be applied to ensure effective vapor dispersal. They may also affect the liquid drained from foam which contributes to LNG vaporization. Several experiments were carried out with high expansion foam with convection and thermal radiation to estimate the foam breakage and liquid drainage from foam. Other experiments were carried out to understand the effects of convection and radiation on foam breakage when foam is applied over a cryogenic liquid. The foam breakage rate, vaporization rates of the cryogen as well as the temperature profile of the vapors through the foam layers were measured. This study aims to understand the effects of convection and radiation on foam breakage, and the liquid drainage from high expansion foam to minimize vaporization of the cryogen and to ensure effective vapor dispersal.

It is important to have high foam stability to ensure that the foam forms a blanket over spilt LNG is effective. Not only does better foam stabilization delay the drainage rate but it reduces the amount of flammable vapors from making their way to the top of the foam allowing for a longer duration of heat exchange between LNG and the foam causing an increase in buoyancy followed by flammable vapors moving to a higher elevation away from ignition sources. Even though tests with exfoliated ZrP have been conducted before and were found to be successful, these experiments were small scale, the foam was generated by vigorous shaking, and the role of ZrP under external conditions such as forced convection and thermal radiation were not studied. This paper focuses on larger lab scale tests utilizing an improved NFPA foam generator and tests foam with and without ZrP under forced convection and thermal radiation. These tests were also performed with and without the presence of a cryogenic liquid spill.

Fire-fighting foams have evolved over the years to better perform their function. They are classified based on their expansion ratios which is the ratio of foam volume to liquid volume. An expansion ration greater than 200 is generally considered to be a high expansion ratio. Although firefighting foams may not be able to fully extinguish a fire alone, they work to suffocate the fire, physically separate the flames from the fuel source, cool the surroundings to which it was applied on, and diminish the ability of any flammable vapors from getting in contact with the air. Foams mainly consists of water, foam concentrate, and may include some form of particle stabilizers. The particle stabilizer

is either a surfactant or a solid particle. [23] The role of a particle stabilizer in foam is to attempt to reduce the surface tension between gas and liquid phase, and there exists an ideal concentration of surfactant called the critical micelle concentration (CMC) at which the surfactant would best perform its function without any excess surfactant or a deficiency in surfactant. [24]

1.3 Zirconium Phosphate nanoplates as foam stabilizers

Studying the stability of foams has been of interest in the past years and this is crucial in the area of mitigating leaked LNG because of its flammability hazard. Researchers focus on the addition of hydrophilic and hydrophobic particles to foam and analyze the effect they have on altering the rate at which the foam breaks and this is through strengthening the attraction of the foam in the air-liquid and liquid-liquid border.[25] Zirconium Phosphate (ZrP) is a thermally stable layered inorganic material with a hexagonal shape whose chemical formula is $Zr(HPO_4)_2*H_2O$.[26] The applications of layered ZrP range from fuel cells, gas sensors, lubricant additives, and flame retardancy[27,28,29,30]. Exfoliating the ZrP introduces more applications such as pickering foams, stabilizing pickering emulsions and liquid crystals.[12] ZrP has been exfoliated previously with agents such as tetrabutylammonium hydroxide (TBA), Propyl Amine and others.[31,32,33,34,35,36] With pickering emulsion of oil-water phase mixtures, exfoliated ZrP nano platelets have been considered to be used as surfactants for stabilized liquid-gas foam.

Experiments with ZrP have been performed by Guevara *et al.* and Zhang to highlight the ability of ZrP to enhance foam stability.[24,16] This study intends to determine the effectiveness of exfoliated ZrP nanoplates in increasing foam stability on a larger scale with the use of a foam generator. Small scale benchtop experiments involving shaking of test tubes to form foam may have non-uniformity in bubble size. A foam generator that builds on the existing NFPA foam generator mode was constructed by Harding *et al.* [37,38] Some of the advantages of the improved foam generator include an adjusted foam application rate suitable for lab use, more mobility due to depending on electric utility only. [39]

Some of the previous studies with different nanoparticles as foam stabilizers were performed utilizing one dimensional nanoparticles. Some examples of these kind of studies include silica spheres while others involve cellulose fibers. However, no studies have been performed on two-dimensional nanoplates with surface modification for foam stabilization. This is a breakthrough exploration and Guevara et al. and Zhang have performed experiments that were found to yield positive results on small scale benchtop experiments. [24,16]

The use of a foam generator in this study will allow the production of uniform bubbles whose sizes may be controlled by passing the foam produced through a mesh. This larger

scale set up will also allow the investigation of the effects of scale up. This foam generator will also ensure that the foam has a high expansion ratio. In this study, experiments with commercially available C2 high expansion foam with a specified concentration of zirconium phosphate exfoliated using TBA were performed and compared with experiments without ZrP. The effect of forced convection and thermal radiation on foam with exfoliated ZrP was determined and compared with foam without ZrP. In addition, studies on a cryogenic liquid spill along with foam and exfoliated ZrP application was studied and compared with foam application without ZrP.

In the literature, foam have been stabilized with one dimensional particles such as silica spheres[40,15], cellulose fibers[35], polymer nanporticles[41], polymer latex particles[42], etc. The main mechanism behind surfactant particles is through the interaction of these particles to form a layer around the foam bubbles adding stability to the foam. The stability of the resulting foam was found to be affected by the shape, viscosity, size, aspect ratio, hydrophobicity, and the concentration of the surfactant particles. [16,43]

In Guevera et al.'s previous work, α-Zirconium Phosphate [$ZrHPO_4)_2$*H_2O, ZrP] was utilized as the particle surfactant. ZrP's well layered structure and existence of OH groups allows it to be easily exfoliated and functionalized. In order to obtain a uniform thickness that exhibits a high aspect ratio, the ZrP is easily exfoliated with tetrabutylammonium

hydroxide (TBA) to form thin monolayers.[44,45] The hydrophobicity is managed by altering the molar ratio of the exfoliating agent to the ZrP molecule itself. The surface area ratio coverage is better in the case of Zrp-TBA for the molecule is two dimensional and this scientifically shows a greater potential than the spherical silica particles and other one dimensional surfactant particles.

Based on previous benchtop results by Lecheng Zhang, ZrP was found to stabilize the foam. The drawbacks from these experiments were that the foam was generated by shaking test tubes vigorously. This leads to a variation between experiments. Therefore, this project will use an improved foam generator model that builds on the NFPA standard for foam generation. These medium scale tests will reduce the unwanted variance present in previous experiments. This foam generator allows for a larger scale experiment that behaves closer to an industry setting foam generator and that is another advantage. The first aim proposed in this project is to compare the stability of high expansion foam (Chemguard) with and without ZrP to see if adding ZrP increases the stability of the foam. A metal mesh is placed under the foam such that only liquid passes through. The liquid passing through the mesh is collected at the bottom of the foam tank that has a sensor measuring weight. The drainage rate is then calculated and compared for the set of experiments with and without ZrP. This drainage rate helps predict how much liquid is drained from the foam over time which plays a crucial role in vaporization of cryogenic liquid when foam is applied over a cryogenic liquid spill.

The second aim proposed in this project is adding cryogenic liquid to the bottom of the tank in the presence of the high expansion foam. A data acquisition system connected to thermocouples is used to measure the temperature at different levels in the foam as to create a temperature profile over different foam heights. This allows the estimation of the temperature of outgoing cryogenic gas. The experiments with cryogenic liquid take place without the metal mesh to estimate the vaporization rate of the cryogenic liquid. Therefore, the vaporization rate of the cryogenic liquid will be obtained from the change in weight on the sensor. These experiments will be performed with and without ZrP to see if adding ZrP increases the stability of the foam.

1.4 Research Objectives of the thesis

Objective 1: Comparing the effect of adding exfoliated ZrP nanoparticles with normal C2 High expansion foam without the presence of forced convection or thermal radiation for the cases of with and without spilt cryogen.

Objective 2: Comparing the effect of adding exfoliated ZrP nanoparticles with normal C2 High expansion foam under forced convection for the cases of with and without spilt cryogen.

Objective 3: Comparing the effect of adding exfoliated ZrP nanoparticles with normal C2 High expansion foam under thermal radiation for the cases of with and without spilt cryogen.

CHAPTER II

EFFECT OF FORCED CONVECTION AND THERMAL RADIATION ON HIGH EXPANSION FOAM USED FOR LEAKED LNG VAPOR RISK MITIGATION

2.1 Overview

Liquefaction of natural gas is an effective way of easily storing and transporting natural gas because of its high ratio of liquid to vapor densities. Any spill of liquefied natural gas (LNG) can result in the formation of a vapor cloud which can not only cause asphyxiation, but can also migrate downwind near ground level because of a density greater than air, and has the potential to ignite. NFPA recommends the use of high expansion foam to mitigate the vapor risk due to LNG. This paper studies the effects of heat transfer mechanisms like forced convection and thermal radiation on high expansion foam breakage with and without a cryogenic liquid. A lab scale foam generator was used to produce high expansion foam and carry out experiments to evaluate the rate of foam breakage, the amount of liquid drained, the vaporization rate of the cryogenic liquid, and the temperature profile through the foam. High expansion foam breakage was found to strongly depend on the amount of forced convection and thermal radiation. Liquid drainage was found to affect the vaporization rate of the cryogenic liquid, especially immediately after foam application. Accounting for external factors like forced convection and thermal radiation can help provide a better estimate for the amount of foam that needs to be applied for effective vapor risk mitigation.

2.2 Materials and Methods

2.2.1 Materials

The foam concentrate used in this work was C2 high expansion foam concentrate by Chemguard. The foam solution was prepared as prescribed by the foam manufacturer (2%).

2.2.2 Experimental method

A foam generator apparatus was designed at the Mary Kay O'Connor Process Safety Center by Harding et al.[39] based on the NFPA standard along with some modifications.[37] These modifications allow lower foam flow rates for experiments in the laboratory, enhanced safety without depending on pressurized air, easier shutdown procedure, smaller pressurized volume negating the requirement of a solenoid valve and a deflector plate for directing the foam to the required location.

2.2.3 Measurement of the foam breakage rate

Foam breakage was estimated by taking photographs of the foam container after specific intervals of time. The images were then analyzed using free image processing software developed by the NIH known as ImageJ.

2.2.4 Mesh setup to measure liquid drainage

To measure liquid drainage, the foam was placed in a container below which a mesh was placed (Fig. 1). As the liquid drained from the foam through this mesh setup, a weighing

balance (Scale WPT/4 300 C7, RadWag, Poland) measured the weight of the falling liquid with time.

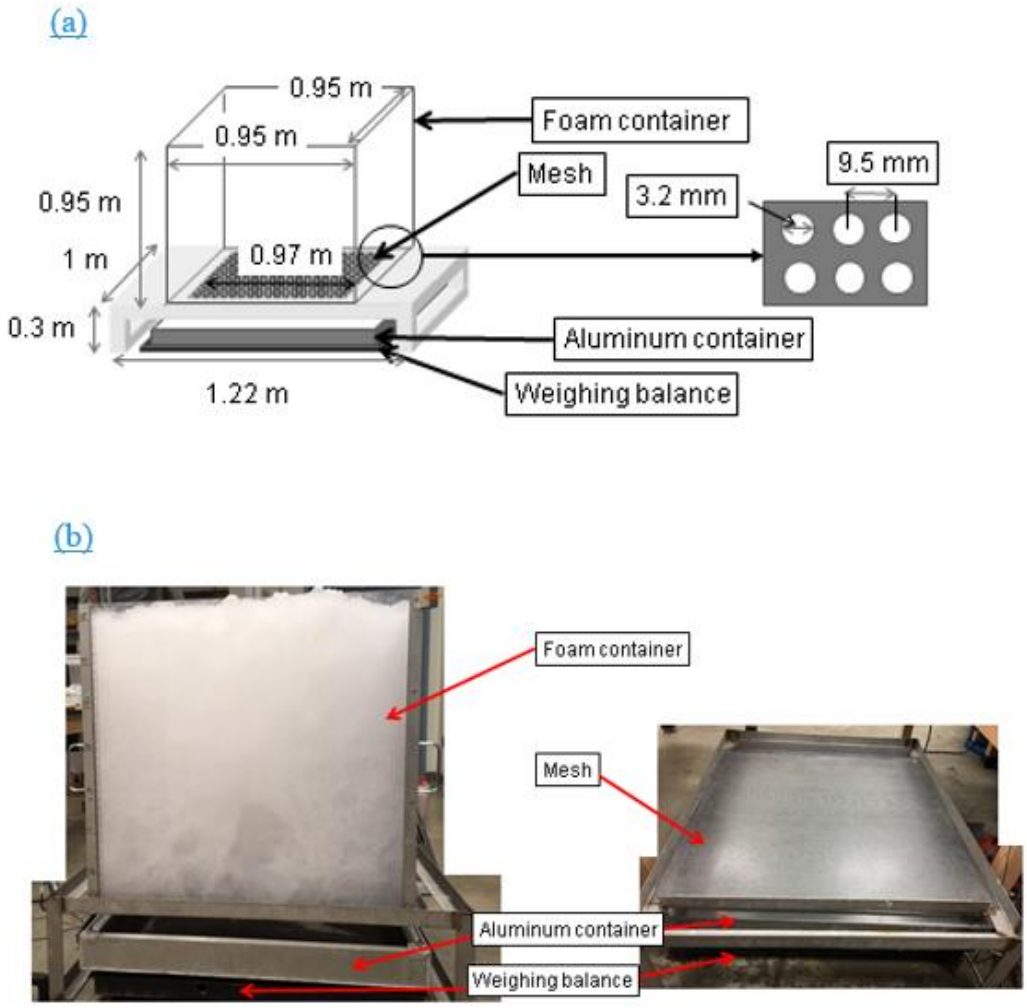

Fig. 1: Mesh setup to measure liquid drainage a) schematic with dimensions b) images of the actual setup

Using the in-house foam generator device, foam was generated and experiments were carried out in the presence of forced convection and thermal radiation.

2.2.5 Wind tunnel setup for experiments under forced convection

A wind tunnel was constructed to minimize the effect of turbulence based on Zhang *et al.* and is shown in Figure 2. A screen was added in the wind tunnel to ensure that the wind velocity is unidirectional. Even though the screen introduced a pressure drop, which limited the magnitude of wind velocities possible, it ensured that the flow was less turbulent. (Mehta *et al*.) Wind was generated using a fan. (Global Industrial, Oscillating Pedestal Fan, 30 Inch Diameter, 1/3HP, 8775CFM). The wind velocities were measured using an anemometer (Omega Engineering, CFMMasterII) and the average of 30 readings has been reported as the average wind velocity. The wind speed is varied by changing the position of the fan and using a transformer to vary the input voltage.

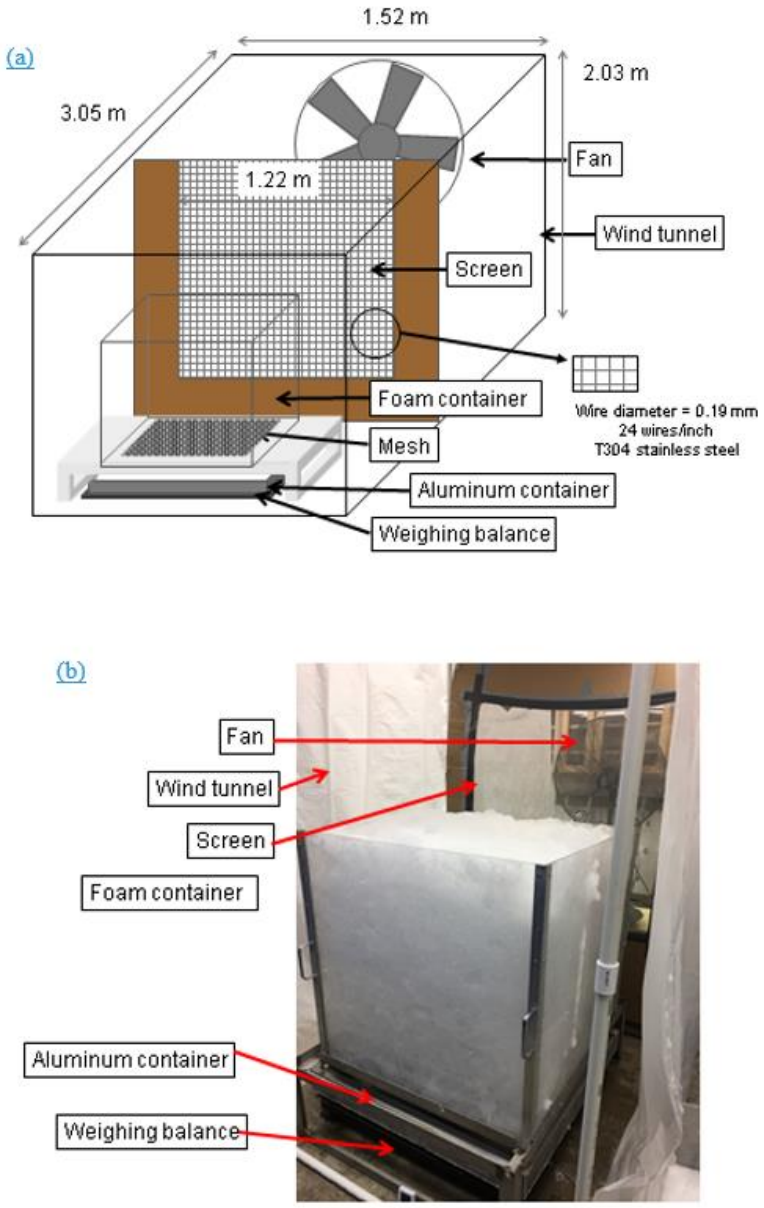

Fig. 2: Wind tunnel setup a) schematic with dimensions b) image of actual setup

2.2.6 Bulb panel setup for experiments under thermal radiation

The bulb panel setup included a frame that was made from slotted angles to which lamp holders (HDX, 150-Watt Incandescent Clamp Light) were attached and is shown in Fig.

3. Nine light bulbs (Philips, 125W, 120V, BR40, Heat Lamp Reflector) were used to produce radiation of required intensities. The thermal radiation intensities were measured with a sensor (Tenmars, TM-206) that can detect up to 2000 W/m^2. The values obtained over a specific area were averaged and reported. The radiation intensities are varied using a transformer to vary the input voltage.

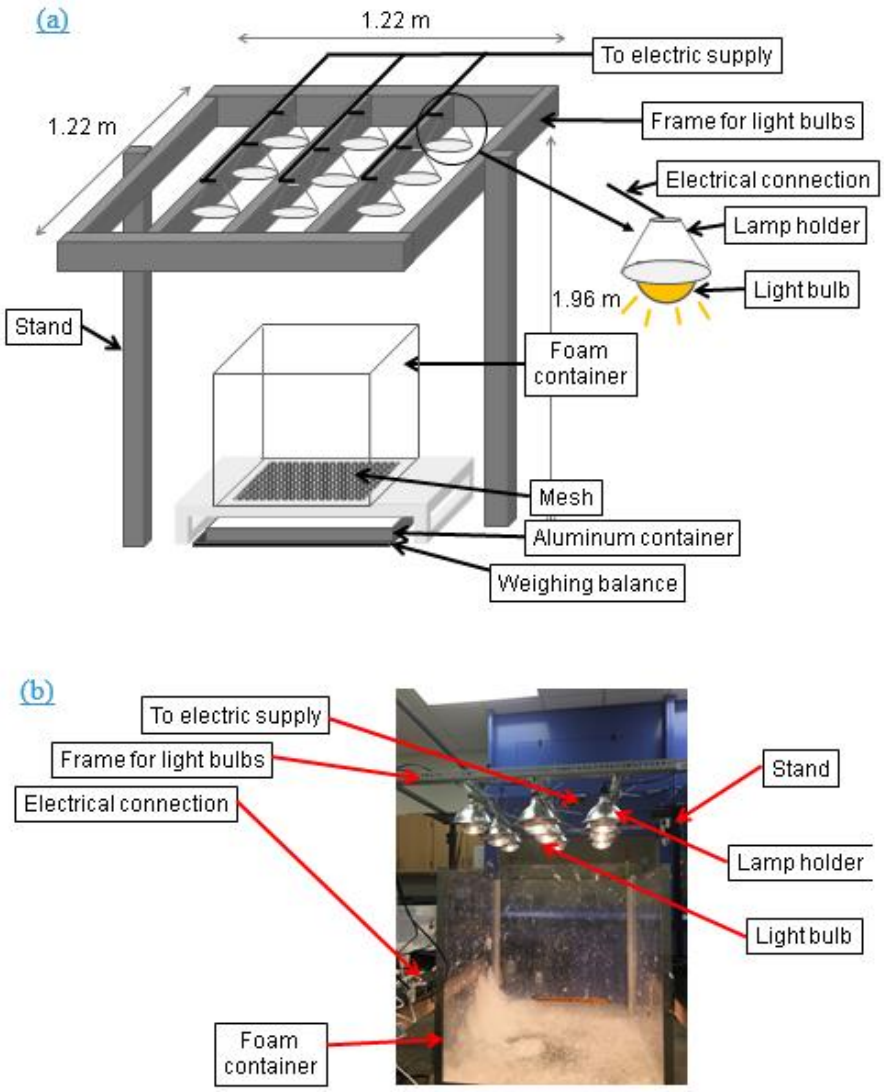

Fig. 3: Bulb panel setup a) schematic with dimensions b) image of actual setup

2.2.7 Setup for experiments with cryogenic liquid

A spill of a cryogenic liquid like LNG contained in a dike was simulated by filling an aluminum container with cryogenic liquid nitrogen. Liquid nitrogen was used for the experiments as it is not flammable, has similar heat transfer properties as LNG, and has been previously used for lab-scale tests. [22,46]

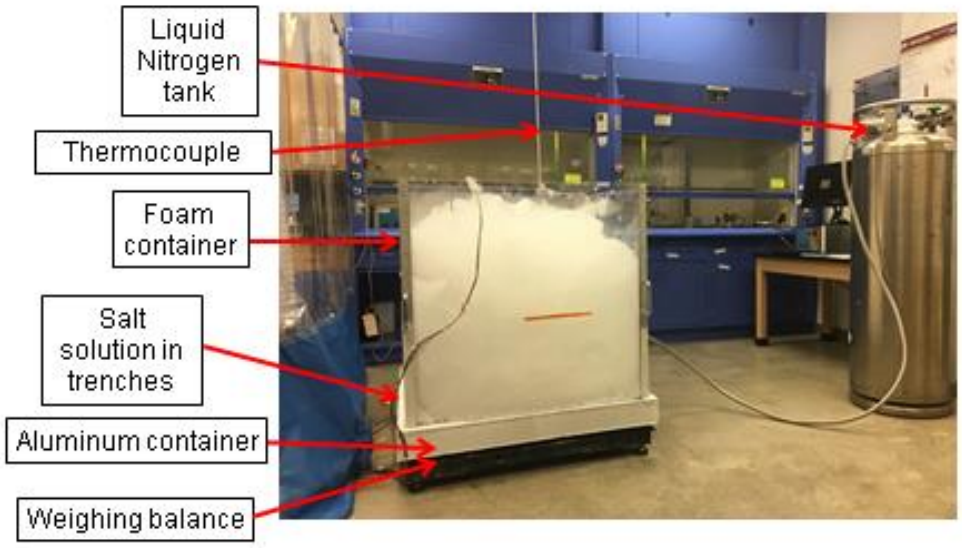

Figure 4: Image showing setup for experiments with liquid nitrogen

The setup used for the cryogenic liquid tests has been shown in the above figure similar to that employed by Zhang et al..[22] The main features of this setup include a weighing balance, an outer aluminum container with trenches to hold a transparent foam container, an inner aluminum container (not shown in figure) to hold the liquid nitrogen. A saturated solution of calcium chloride (83-87%, McMaster Carr) was prepared and added in the

trenches to create a liquid seal, blocking the flow of liquid nitrogen vapors through it, and allowing a freezing point depression due to the presence of salt.

Approximately 35 kilogram of liquid nitrogen was filled in each experiment through a circular perforation made on the side of the foam container. Foam was filled around 5 minutes after all the liquid nitrogen had been filled in the container. Images were captured to record the foam height using a recording device and analyzed using ImageJ. The temperature of the room and humidity during the experiment were also recorded. The temperature of the foam and outgoing vapor were measured using six thermocouples (Type T, TJC300 series, Omega Engineering) with a distance of 0.18m between each of them. The thermocouple setup has a unique design, and was first used by Zhang *et al.* It allows the measurement of the foam and vapor temperature simultaneously using an upward thermocouple which is largely influenced by the foam temperature and a downward thermocouple which is predominantly affected by the temperature of the outgoing vapor.

2.3 Experimental Results

2.3.1 Expansion ratio of foam

To determine the expansion ratio of foam, experiments were carried out filling the foam container placed on the weighing balance and measuring the weight of the foam added. By estimating the volume of the foam in the container and the weight, the expansion ratio

may be calculated. The average expansion ratio calculated from five trials was found to be 420 ± 35.

2.3.2 Foam breakage rate and liquid drainage measurement

Foam breakage rate helps estimate when foam needs to be applied to replenish an existing layer of foam, to ensure that the outgoing vapor of the cryogenic liquid is lighter than air, for better vapor dispersal. The foam breakage rate is calculated by measuring the foam height over time and then estimating the foam breakage rate. Liquid drainage from foam can affect the rate of LNG vaporization from a spill as it determines the "boil-off" effect from foam. If the liquid drainage from foam is too high, then the amount of vapor generated due to foam application may be significantly higher. Therefore, this work aims to study the effect of this liquid drainage on the LNG vaporization. Experiments were carried out with the mesh setup to estimate the liquid drained from foam under varying conditions of forced convection and thermal radiation.

2.3.3 Foam breakage and liquid drainage without forced convection or thermal radiation

Experiments without forced convection and only background thermal radiation have been illustrated in Fig. 5. They are used as a control in this study, to measure the variation between experiments with and without forced convection and radiation. The foam breakage rate was estimated by fitting foam height vs. time data and estimating the slope

of the graph. This experiment was repeated three times and the average slope has been shown in the table below.

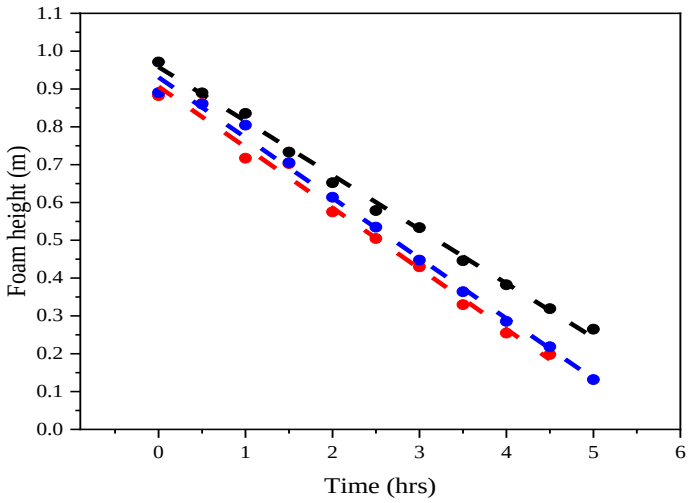

Fig. 5: Foam height vs time without forced convection or radiation

The Table below shows the foam breakage rate without forced convection or radiation for the high expansion foam.

Table 2: Foam breakage rates without forced convection or radiation

Experiment	Foam breakage rate	R^2
1	0.143 ± 0.003	0.996
2	0.160 ± 0.005	0.991
3	0.159 ± 0.004	0.995
Average	0.154 ± 0.004	

The liquid drainage rates for these experiments were also quite consistent and have been show in Fig. 6.

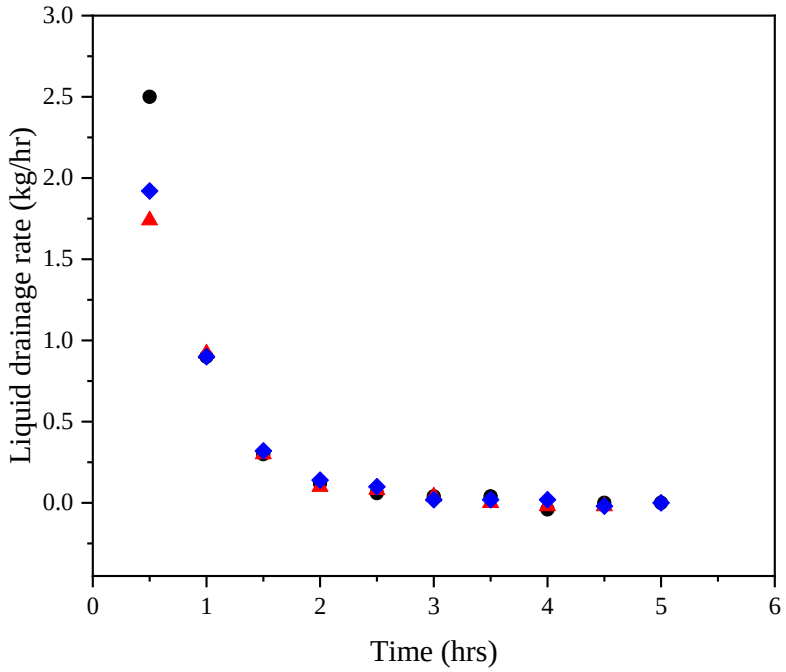

Fig. 6: Liquid drainage vs time without forced convection or radiation

2.3.4 Foam breakage and liquid drainage under forced convection

Average wind speeds in the wind tunnel were determined using an anemometer. The values obtained have been shown in Table **3**

Table 3: Measured average wind speeds

Experiment	Measured average wind speed (m/s)
1	0.4 ± 0.01
2	0.9 ± 0.08
3	1.3 ± 0.06
4	1.9 ± 0.5
5	2.1 ± 0.7
6	2.4 ± 0.5
7	2.5 ± 0.4

Experiments with forced convection showed how the foam height reduced with time and this has been illustrated in Fig. 7 which helped determine the foam breakage rate at different wind velocities. The foam breakage rate was estimated by adding a linear fit to the foam height vs. time data and calculating the slope for each fit. The values for these slopes along with the standard deviations and R^2 have been shown in Table **4**4. The results clearly demonstrate the effect wind has on foam breakage. Increasing the wind speed can significantly alter the foam breakage rate. When compared with no forced convection, the maximum breakage rate at 2.5 m/s was found to be 0.5 m/hr which is more than three times faster than the foam breakage without forced convection. The figure below shows the foam height vs time under forced convection.

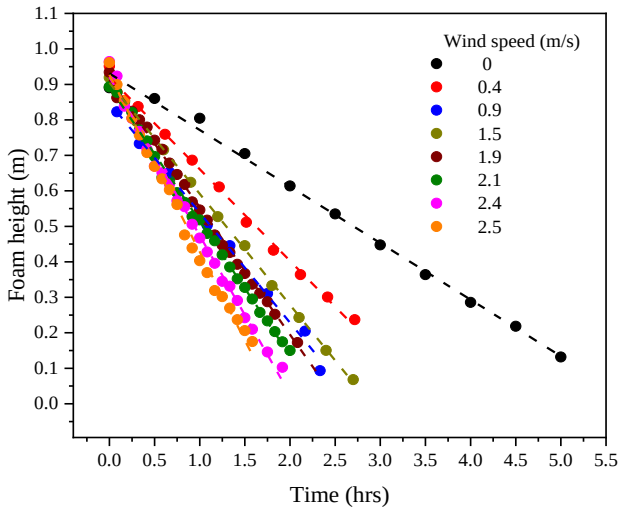

Fig. 7: Foam height vs time under forced convection

Table 4: Foam breakage rates at different wind speeds

Average wind speed (m/s)	Foam breakage rate (m/hr)	R^2
0	0.158 ± 0.004	0.993
0.4	0.258 ± 0.004	0.997
0.9	0.309 ± 0.009	0.993
1.3	0.313 ± 0.003	0.999
1.9	0.359 ± 0.004	0.997
2.1	0.368 ± 0.004	0.996
2.4	0.447 ± 0.007	0.995
2.5	0.500 ± 0.01	0.993

In addition, the foam breakage rate vs wind speed has been shown in Fig. 8 and shows the variation of foam breakage rate with wind speed. This gives an estimate of foam breakage rates under different wind speeds which can help estimate when foam needs to be applied to ensure vapor dispersal.

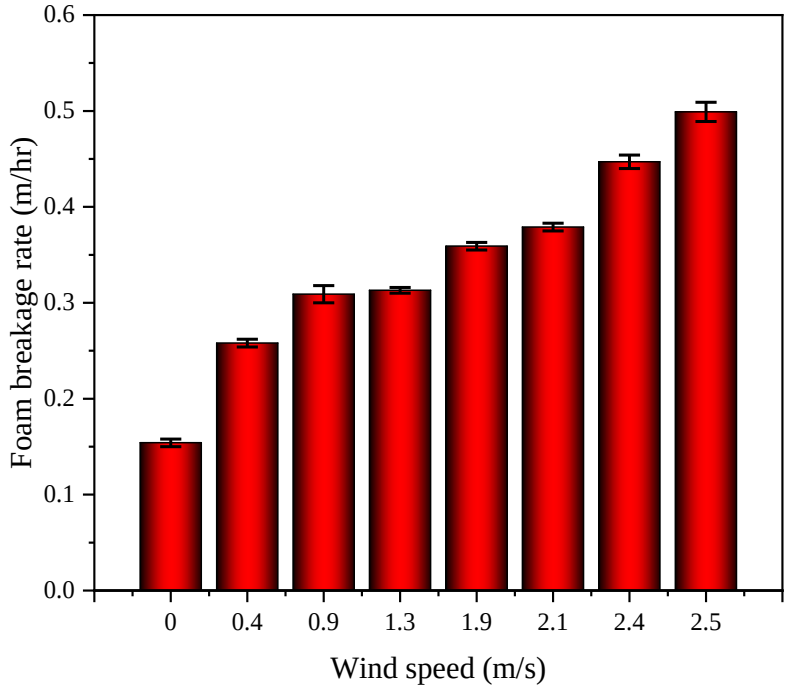

Fig. 8: Foam breakage rate vs. average wind speed

The liquid drainage under forced convection was also obtained from the mesh setup. The foam applied on the mesh drained liquid over time and the amount of liquid drained was measured using a weighing balance. The liquid drainage rate is the amount of liquid

drained over a specific interval of time. The liquid drained over five minutes was calculated and the drainage rate was plotted as a function of time and is shown in Fig. 9.

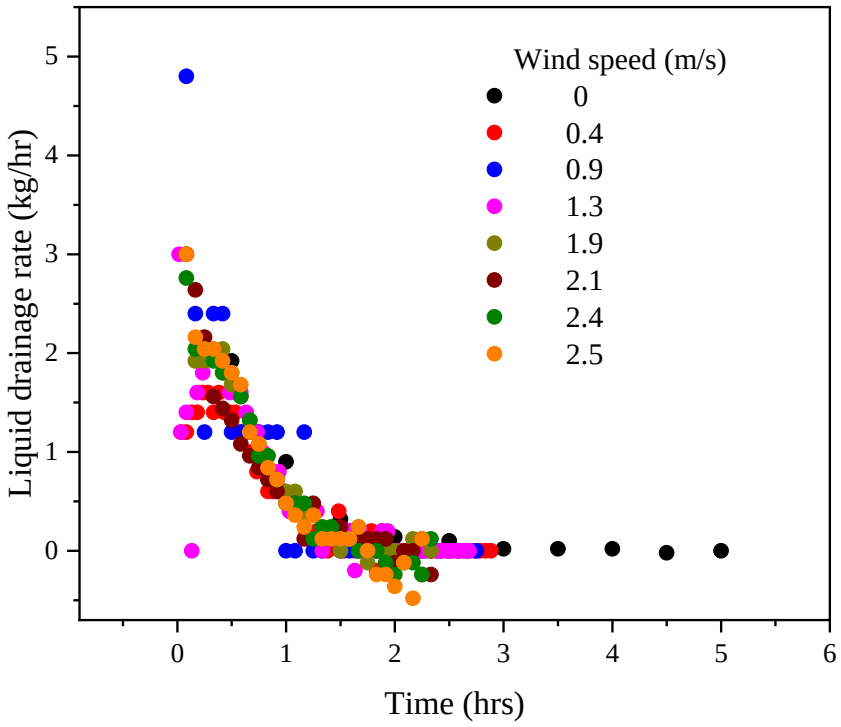

Fig. 9: Liquid drainage rates under forced convection

It is easily observed that the liquid drainage rate in all cases is quite similar. This possibly indicates that the water being drained from the upper layers of the foam might be retained by the lower layers, maintaining a uniform liquid drainage rate independent of wind speed. It is important to note that the water drainage may be affected by several factors including the initial height of the foam, the humidity, and the evaporation of water in the presence of forced convection.

2.3.5 Foam breakage and liquid drainage under thermal radiation

Different radiation intensities were measured using a radiation sensor. As the radiation intensities varied with height, the foam breakage and liquid drainage from the top (0.95 m) till 0.84 m were estimated and used for data analysis. Ten readings of radiation intensities in this height were averaged and have been reported in the table below.

Table 5: Measured average radiation intensities over the top four inches of the foam container

Experiment No.	Measured average radiation intensity (W/m^2)
1	60 ± 12
2	140 ± 25
3	200 ± 33
4	270 ± 50

Experiments with different intensities of thermal radiation showed have been illustrated in Fig. 10. Since the foam breakage was measured as the foam height reduced from 0.95 m to 0.84m, to maintain uniform radiation intensity, the time period for such measurements was much shorter than the experiments with forced convection and without forced convection and radiation. The foam breakage rates estimated in these experiments are the initial rate of foam breakage and not steady state. The liquid drainage rate was found to be nearly constant, at each radiation intensity over this short time period. It should

be noted that the standard deviation was high in these calculations; therefore, no quantitative conclusions may be drawn from this data set. The effect of increasing radiation intensity on foam breakage has been shown in foam breakage rate was estimated by adding a linear fit to the foam height vs. time data and calculating the slope for each fit. The values for these slopes along with the standard deviations and R^2 have been shown in. The results clearly demonstrate the effect radiation has on foam breakage, highlighting that increasing the radiation intensity increases foam breakage.

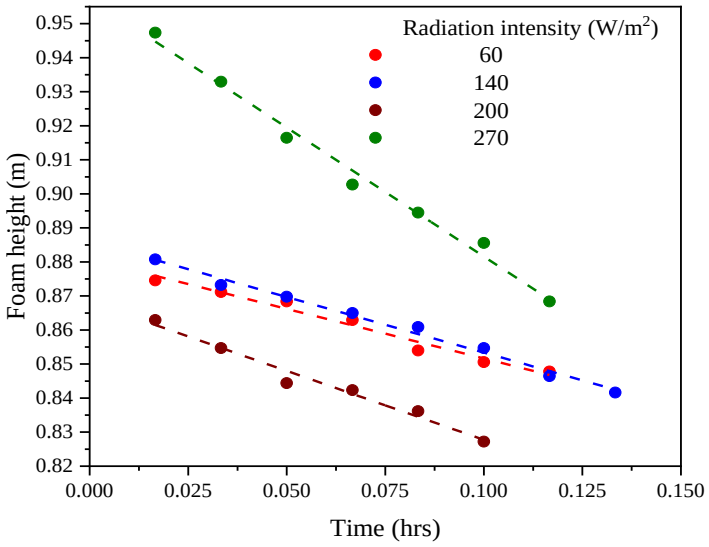

Fig. 10: Foam height vs time for different radiation intensities

The table below shows the foam breakage rate under different radiation intensities for the foam.

Table 6: Foam breakage rates at different radiation intensities

Radiation intensity (W/m^2)	Foam breakage rate (m/hr)	R^2
60	0.29 ± 0.02	0.974
140	0.33 ± 0.01	0.990
200	0.41 ± 0.02	0.985
270	0.76 ± 0.04	0.989

The figure below shows the foam breakage rate for the different thermal radiation intensity values experimented.

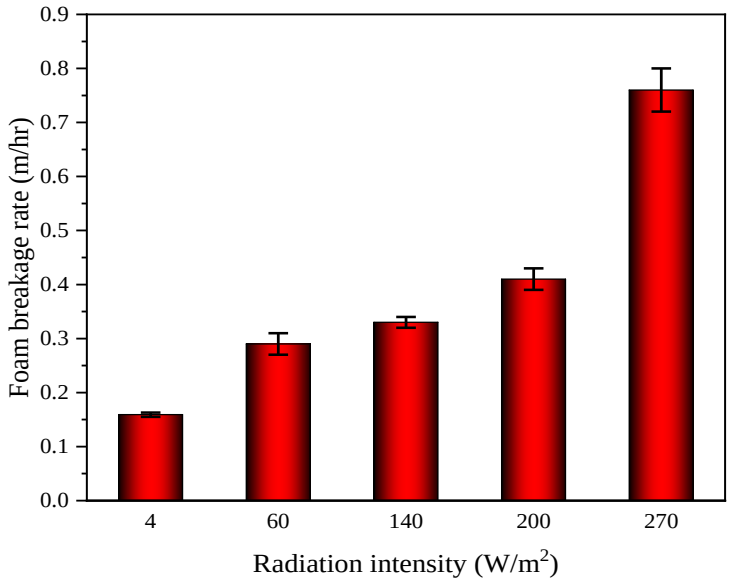

Fig. 11: Foam breakage rate vs radiation intensity

The table below provides the liquid drainage rate values obtained for the different thermal radiation intensity experiments.

Table 7: Liquid drainage rates at different radiation intensities

Radiation intensity (W/m^2)	Liquid drainage rate (kg/hr)
60	1.7 ± 0.2
140	2.8 ± 0.9
200	3.4 ± 0.8
270	3.7 ± 0.7

2.4 Experiments with liquid nitrogen

2.4.1 Foam breakage rate with liquid nitrogen

Foam height vs time, with and without liquid nitrogen, for three cases, without forced convection or radiation, with forced convection and with radiation have been shown in the figure belowError! Reference source not found.**.** It can be clearly observed from these figures that the foam breakage with liquid nitrogen is faster in all three cases, and this can be attributed to the effect of cryogenic liquid interaction with the foam.

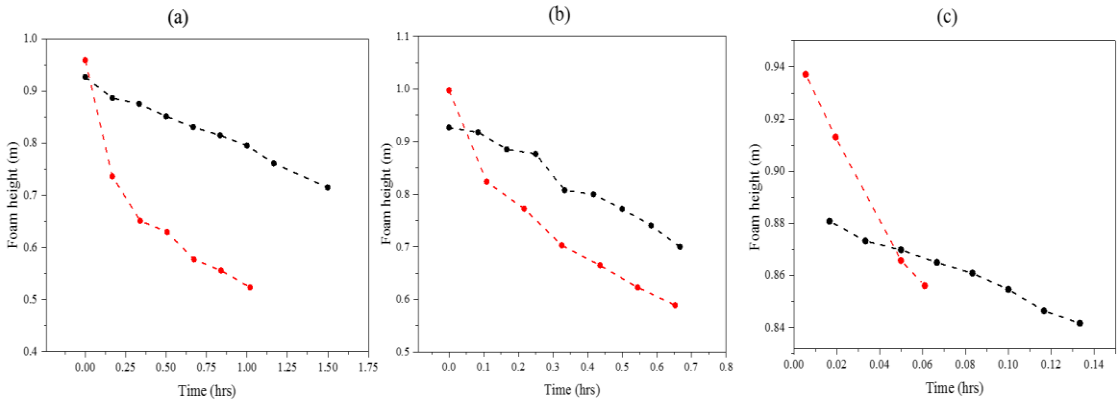

Fig. 12: Foam breakage vs time under a) without forced convection or radiation b) forced convection and c) radiation. Without LN_2 (black), with LN_2 (red)

Foam height vs time, with and without liquid nitrogen, for three cases, without forced convection or radiation, with forced convection and with radiation have been shown in the above figureError! Reference source not found.**.** It can be clearly observed from these figures that the foam breakage with liquid nitrogen is faster in all three cases, and this can be attributed to the effect of cryogenic liquid interaction with the foam.

2.4.2 Vaporization rate without forced convection or radiation

The vaporization rate with liquid nitrogen was measured by obtaining the difference in weight of the container over time. The vaporization rate without forced convection and thermal radiation has been shown in Fig.12. The liquid drainage rate has also been shown in the same figure and shows how the liquid drainage influences the rate of vaporization of the cryogenic liquid. Once the liquid drainage falls below 2 kg/hr, the vaporization rate stabilizes and is primarily influenced by conduction through the container. The steady

state vaporization rate is similar to that obtained by Zhang et al., which was close to 11 kg/hr. [22]

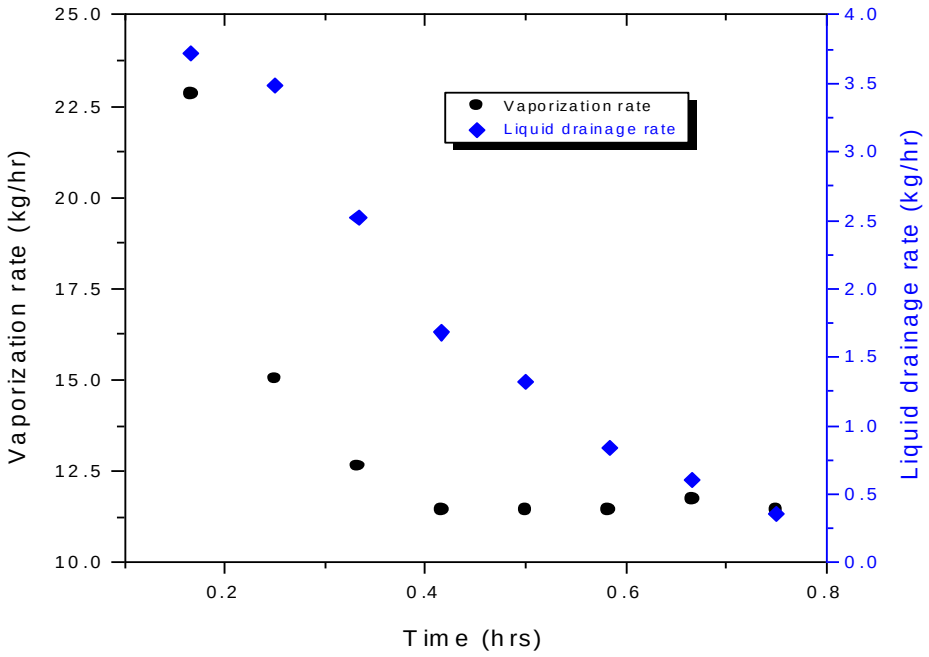

Figure 13: Vaporization rate and liquid drainage without forced convection or radiation

2.4.3 Foam breakage rate and vaporization rate with forced convection

The following figure shows the foam height vs time when foam was applied over liquid nitrogen at different wind induced convection values.

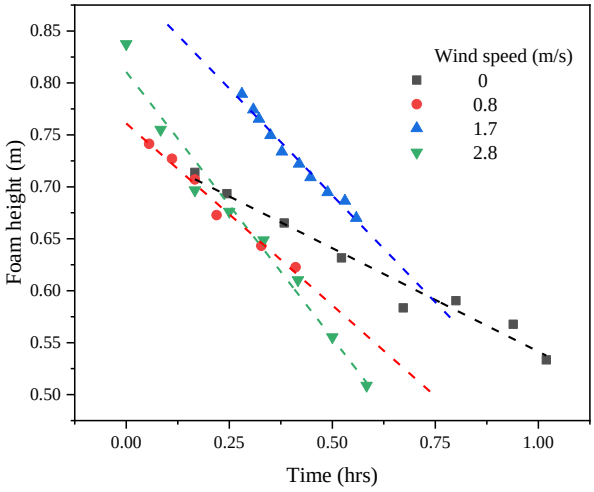

Figure 14: Foam breakage rate vs time for foam under different wind induced convection values in the presence of LN_2

The following table shows the percentage difference in foam breakage rates, between using foam with ZrP and without ZrP under forced convection.

Table 8: Foam breakage rate vs time under different wind induced convection values in the presence of LN_2 along with the performance ratio

Wind speed (m/s)	Foam breakage rate (kg/hr)
0	0.199 ± 0.015
0.8	0.350 ± 0.024
1.7	0.411 ± 0.019
2.8	0.513 ± 0.034

The vaporization rate with forced convection has been shown in Fig.13 along with liquid drainage from the foam under similar conditions. This graph also shows that once the liquid drainage falls below 2 kg/ hr, it does not significantly contribute to the vaporization rate of the cryogenic liquid.

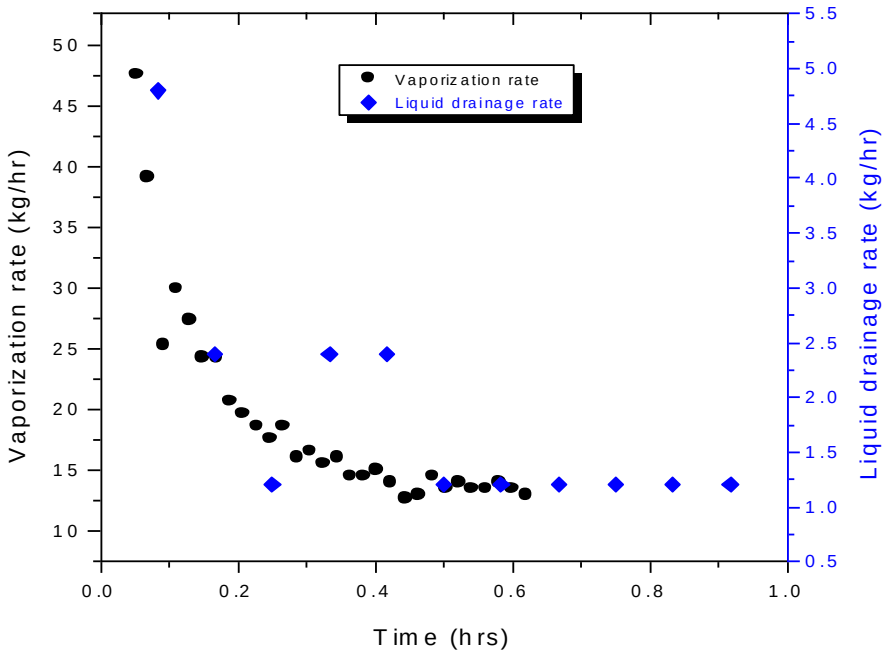

Figure 15: Vaporization rate and liquid drainage with forced convection. The vaporization rate was calculated when the wind speed was 0.9 m/s while the liquid drainage was calculated at a wind speed = 0.8 m/s

2.4.4 Foam breakage rate and vaporization rate with thermal radiation

The following figure shows the foam height vs time when foam was applied under different thermal radiation intensities in the presence of LN_2.

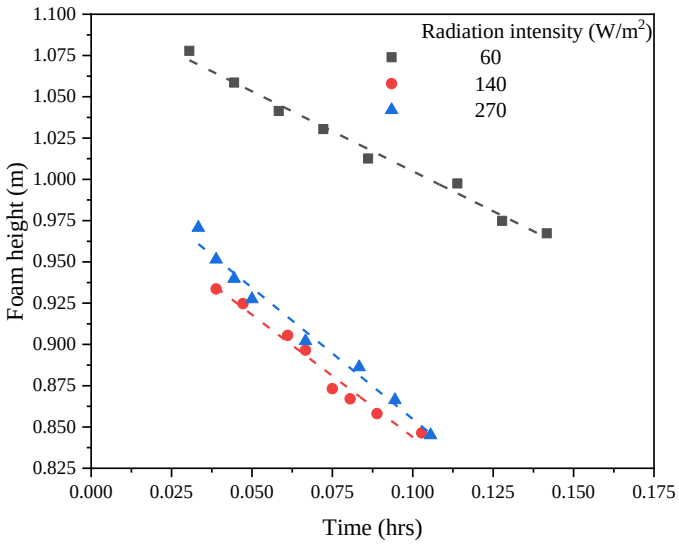

Figure 16: Foam breakage rate vs time for foam under different thermal radiation intensity values in the presence of LN_2

The following table summarizes the foam breakage rates with liquid nitrogen, with foam application under thermal radiation.

Radiation intensity (W/m^2)	Foam Breakage Rate (kg/hr)
4	0.199 ± 0.015
60	0.968 ± 0.044
140	1.482 ± 0.096
270	1.591 ± 0.084

As the radiation data was collected from only for the foam breakage until the foam height reached 0.85 m, it was not possible to obtain the steady state vaporization rate or liquid

drainage. The initial mean vaporization rate was found to be 31 ± 4 kg/hr and the initial mean liquid drainage was around 2.8 ± 0.9 kg/hr.

2.4.5 Temperature profile with liquid nitrogen

The temperature profile was measured in these experiments to explain the ability of the foam to exchange heat with the outgoing vapor of the cryogenic liquid and decrease its density, thereby ensuring effective vapor dispersal. The temperature profile without forced convection and thermal radiation has been studied by Zhang *et al.*.[22] In this article, we studied the temperature profile under forced convection and radiation and have been shown in Fig. 14 and Fig. 15 respectively.[22]

The unique design of the thermocouple setup allows the measurement of the foam and vapor temperature simultaneously. The upward thermocouple which is mainly affected by the foam temperature and a downward thermocouple primarily indicates the temperature of the outgoing vapor. As expected, the temperature of the outgoing vapor measured by the downward thermocouple was found to be lower than that of the foam. As the vapor rises up through the foam, heat is transferred from the foam to the vapor, increasing its temperature and decreasing its density.

2.4.6 Temperature profile with forced convection

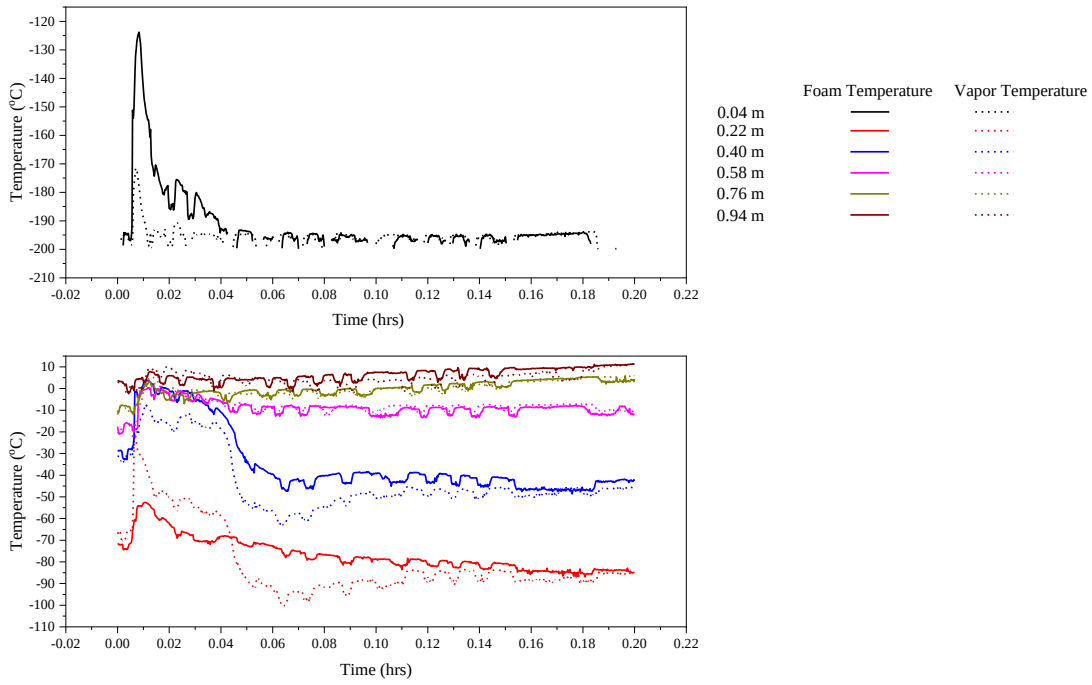

Figure 17: Temperature profile under forced convection (wind speed=0.8 m/s)

2.4.7 Temperature profile with thermal radiation

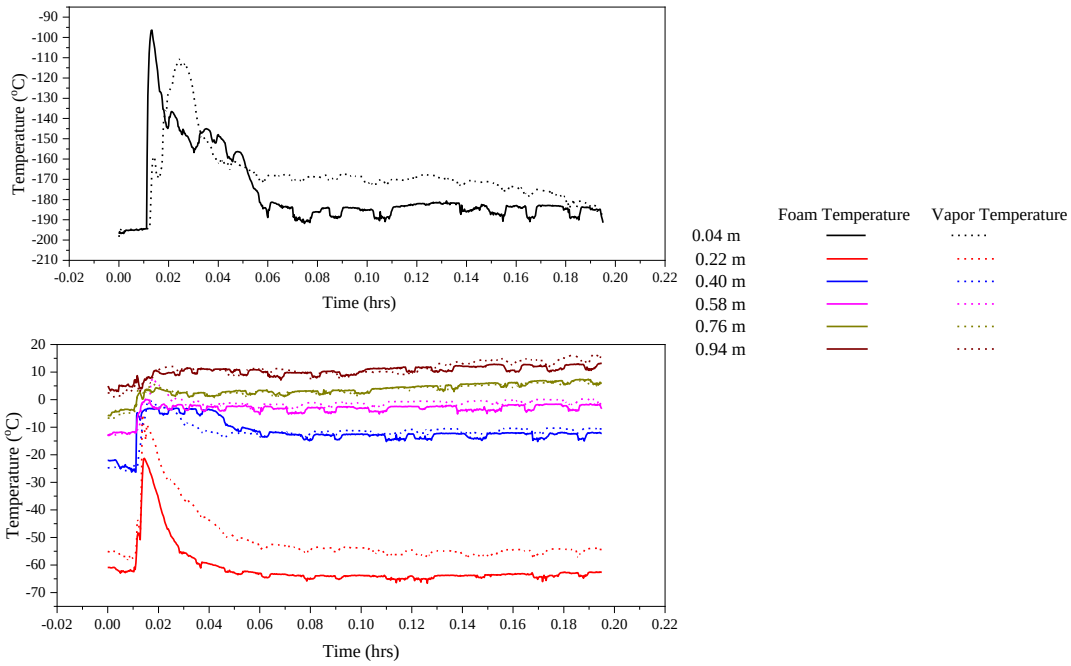

Figure 18: Temperature profile under thermal radiation (radiation intensity = 80 W/m^2)

2.5 Discussions

2.5.1 Mechanism of foam breakage

It is clear from the results obtained that forced convection and thermal radiation influence the rates of foam breakage. However, identifying the mechanisms behind which factors affect foam breakage and liquid drainage will give a better understanding of how forced convection and thermal radiation affect foam breakage.

Pugh has listed out the phenomena destabilizing the foam. These may include liquid drainage, Ostwald ripening, evaporation, coalescence, and external disturbances. All these mechanisms can contribute to making foam less stable and ultimately causing its breakage. Liquid drainage is the liquid that gets drained out of the foam due to gravity. The loss of liquid from foam can significantly affect its effectiveness. [12]If more liquid drains out of the foam, it can significantly increase the rate of vaporization of LNG, especially before an ice layer gets formed. External disturbances include natural convection, forced convection or radiation. Zhang et al. found that foam application can significantly reduce the heat flux due to natural convection, forced convection and radiation which contribute to vaporizing cryogenic liquids.[22] However, it is important to understand the affect of these external disturbances on foam breakage itself to ensure that the foam forms a blanket that remains stable for a longer period.

Ostwald ripening is the coarsening of bubbles due to the diffusion of air from one bubble to another over time to attain thermodynamic equilibrium. Smaller bubbles tend to lose gas and become smaller and eventually disappear while larger bubbles grow over time. This eventually increases the average size of bubbles.[23] Evaporation due to convection and radiation can decrease the critical liquid fraction of bubbles in the upper layers of the foam. Carrier and Colin found that when the liquid fraction drops below a critical value, bubbles tend to break.[47] Li et al. also performed experiments verifying the influence of environmental humidity on foam stability and found that change in humidity can significantly alter foam stability.[48] Thus, it is possible for evaporation to affect the stability of foam. Coalescence can also influence the rate of foam breakage. Coalescence occurs due when the film separating two bubbles breaks. This can be a cooperative process resulting in a series of rupture of many bubbles.[47,23] Coalescence observed in foam may be different from that observed in isolated thin films and its mechanism is not very well understood.

External disturbances include natural convection, forced convection or radiation. Zhang *et al.* found that foam application can significantly reduce the heat flux due to natural convection, forced convection and radiation which contribute to vaporizing cryogenic liquids.[22,49] A schematic combining these factors resulting in foam breakage has been shown in Fig. 16.

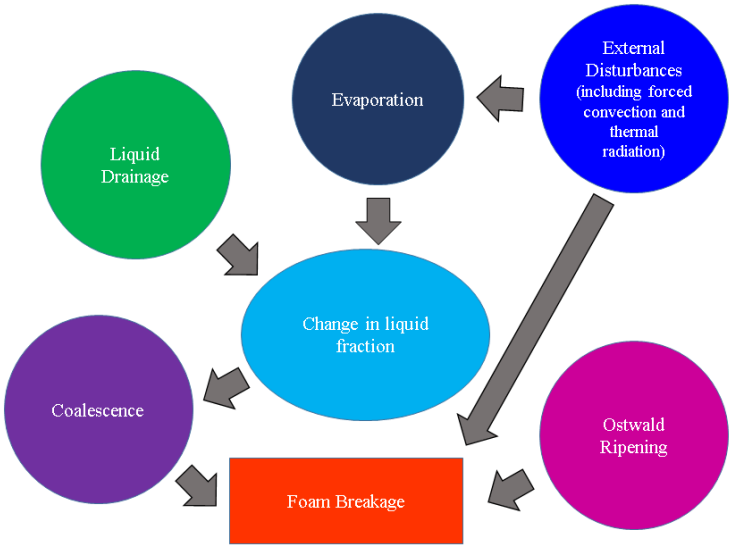

Figure 19: Schematic showing the mechanism of foam breakage

While all these phenomena can destabilize foam, it is important to estimate their effect on foam breakage to identify factors that may be controlled in order to minimize foam breakage. It is important to note that several factors may be dependent on each other and may exhibit synergistic effects.

2.5.2 Liquid drainage from foam

The liquid drainage from foam may play a crucial role in vaporization of LNG, especially when the boil-off effect is significant, immediately after the foam is applied. The liquid drainage from the foam predicted by these experiments can be compared with a theoretical model made by Conroy *et al.* which predicts the height of the drained liquid from high expansion foam. The calculations for the model have been explained in the supplementary

section. A comparison of the model to the experimental result without forced convection and thermal radiation has been shown in Fig. 17. The model seems to agree with the experimental result and shows similar trends.

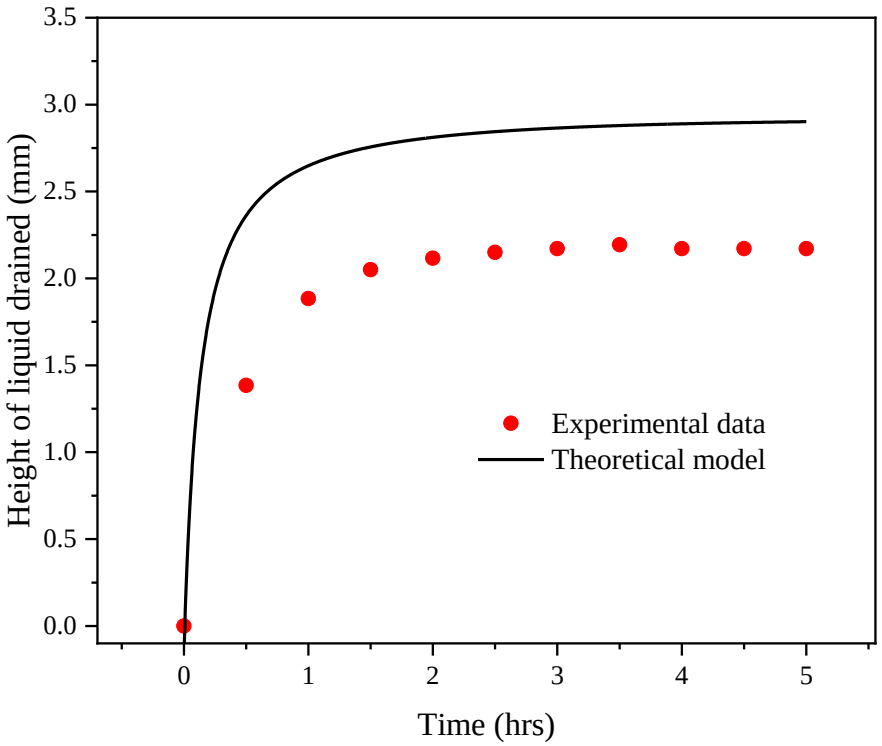

Figure 20: Liquid drainage vs time without forced convection or thermal radiation obtained experimentally compared to that obtained from the theoretical model

2.5.3 Warming effect of the foam through the foam

The temperature of the outgoing vapors through the foam have been measured experimentally and shown in Fig 14 and 15. As long as the foam height is maintained sufficiently high, the vapors should be heated to a point, where its density is lower than

that of surrounding air and can be dispersed easily. Fig. 18 shows the temperature at which density of methane (major component of LNG vapor) becomes equal to that of the surrounding air at 25 ^{o}C. This occurs at nearly -105.7 ^{o}C. Therefore, as long as the vapor temperature is above this, it should be reasonable to assume sufficient dispersal. In this experimental study, liquid nitrogen was used but based on work by Takeno *et al.* simple calculations may be performed to estimate the vaporization rates of LNG, and the vapor temperature predicted by experiments using liquid nitrogen is usually lower than that for LNG making the estimates more conservative.[46]

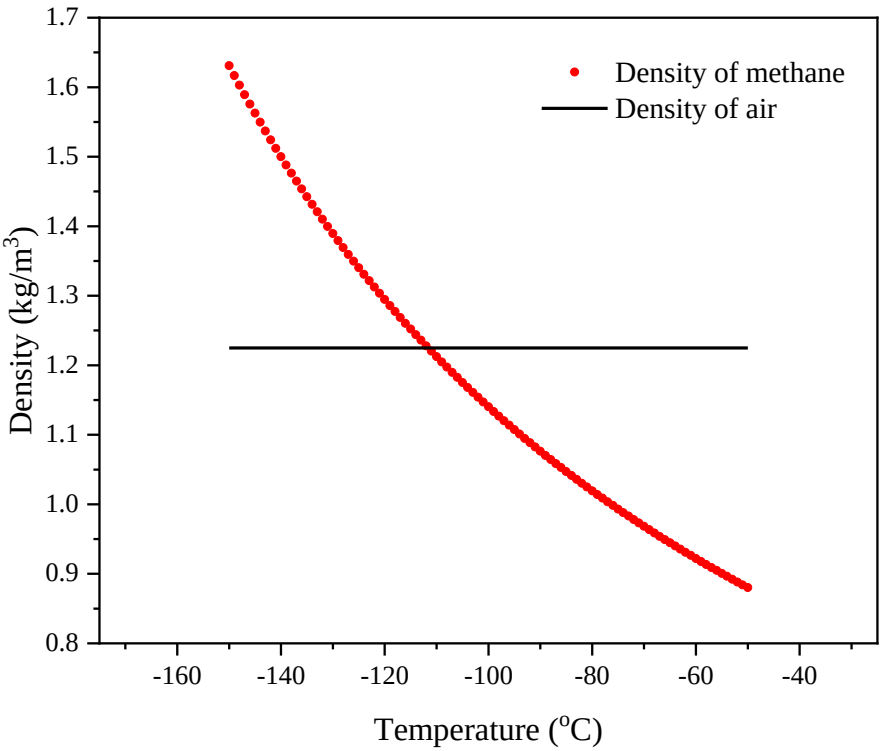

Figure 21: Density of methane as a function of temperature, methane density is equal to air density (at 25 ^{o}C) at about -105.7 ^{o}C.

2.6 Conclusion

High expansion foam can not only help reduce the heat transfer to LNG through convection and radiation for reduced vaporization, but also heats up LNG vapor that passes through the foam layers, enabling ease of dispersal for risk mitigation. However, foam drains liquid over time which can increase the vaporization of LNG. A lab scale foam generator was used to produce high expansion foam and study foam breakage and liquid drainage with time. The effects of external factors like forced convection and thermal radiation on foam breakage were studied. It was found that both forced convection and thermal radiation can have a significant effect on the rate at which foam breaks. The rate at which liquid drains from the foam have also been determined under different conditions of forced convection and thermal radiation. Tests with liquid nitrogen show that the foam can help lower the vaporization rate of the cryogenic liquid. External factors like forced convection and thermal radiation can affect the rate of foam breakage, and must be accounted for while estimating the amount of foam that is applied over cryogenic liquid spills.

Previous work in this area covered only one windspeed, thus no model can be given from that dataset that could potentially predict the behavior of foam breakage under higher/lower windspeeds. The experiments conducted in this research measured the effect

from eight different windspeeds ranging from 0 m/s to 2.5 m/s, hence a trend towards predicted how the behavior of foam would change with varying windspeeds.

Previous work in this area covered only one thermal radiation intensity, thus no model can be given from that dataset that could potentially predict the behavior of foam breakage under higher/lower thermal radiation intensity. The experiments conducted in this research measured the effect from eight different wind speeds ranging from 3 w/m^2 till 270 w/m^2, hence a trend towards predicted how the behavior of foam would change with varying thermal radiation intensities.

The further modified setup used for the experiments of this research allowed measurement of liquid drainage at the same time with the foam breakage rate and this is crucial in order to better predict how the water draining from the foam effects the boil-off effect of leaked LNG. The previous setup did not include a method to measure liquid drainage and the foam tank used was very tall (around 2m); thus, this might not accurately represent industrial scenario regarding gravity.

CHAPTER III

STABILIZING HIGH EXPANSION FOAM USED FOR LEAKED LNG VAPOR RISK MITIGATION USING ZIRCONIUM PHOSPATE NANOPLATES

3.1 Overview

Natural gas has been an evolving industry for its numerous advantages over other energy sources such as coal. Natural gas is often stored in its liquid form as liquefied natural gas (LNG) because it has a much lower liquid volume. The National Fire Protection Agency (NFPA) as well as the American Gas Association (AGA) recommends high expansion foam use to mitigate the risk due to a cryogenic vapor cloud which may result from any leaked LNG. This paper studies the role of exfoliated Zirconium Phosphate (ZrP) nanoplates in stabilizing high expansion foam. Experiments performed with ZrP nanoplates show that they can improve foam stability even in the presence of external forces like forced convection and radiation. (Results) Experiments carried out in the presence of a cryogenic liquid spill along with the ZrP stabilized foam highlights its effectiveness in mitigating the vapor risk of LNG.

Innovations in hydraulic fracturing techniques have accelerated natural gas production, and this is expected to increase even further over the next few decades. Pipelines may not always be the best form of transportation of natural gas, especially over long distances. Therefore, it is compressed and cooled to its liquid form in which its density is 600 times

that of its vapor. While tis may be an easy way to transport it, a leak of LNG can form a vapor cloud which remains close to the ground level due its high density at low temperatures. This vapor cloud can ignite if it finds an ignition source. High expansion foam may be used as a mitigation technique to reduce the vapor risk of any leaked LNG.

3.2 Materials and Methods

3.2.1 Materials

Chemguard C2 high expansion foam purchased from Chemguard Inc. Zirconium Phosphate ($(Zr(HPO_4)_2 \cdot H2O$) was purchased from Sunshine Factory, Tetrabeutylammonium hydroxide ($C_{16}H_{37}NO$) was purchased from Sigma-Aldrich. Liquid nitrogen was used instead of LNG as a cryogenic liquid due to similarity in properties and due to its non-flammable nature for lab safety.

3.2.2 Exfoliation of ZrP with TBA

ZrP was bought from the supplier thus no need for synthesizing ZrP. The mixture will include 20 grams of ZrP along with 44 grams of TBA and 400 mL of water. For the purpose of better exfoliation the mixing will take place on a smaller scale. Every gram of ZrP needs a corresponding 2.2 mL of TBA for exfoliation. Therefore, 2 grams of ZrP along with 4.4 grams 40 mL of water were weighed and added to a centrifuge tube. This step is done ten times. The ten centrifuge tubes are then placed on a vortex for 2 minutes each to allow for mixing. They are then placed to centrifuge such that the denser unexfoilated ZrP is gathered at the bottom. The contents are separated from ten

unexfoilated ZrP and placed on a sonicator for an hour. The centrifuge tubes are left to rest. The next day the contents from the ten centrifuge tubes are transferred to a 500 mL pyrex bottle and is now ready to be used for experiments.The figure below highlights the interclation process of exfoliating ZrP with TBA.

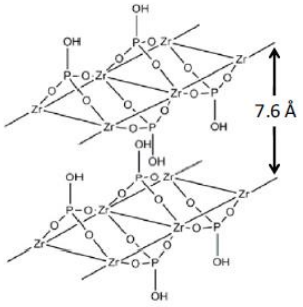

A. α-ZrP

B. TBA

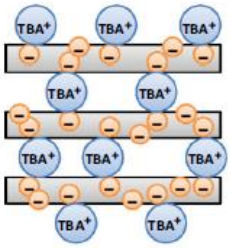

C. Intercalation between ZrP

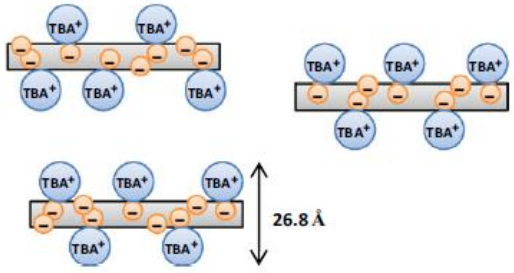

D. Exfoliated monolayer ZrP-TBA

Figure 22: Exfoliation process of ZrP with TBA: ZrP and TBA are placed in the same flask and allowed to mix. C. Intercalation between ZrP and TBA molecules occur. D. ZrP layers break forming monolayer ZrP structure that can be further functionalized as needed. [50]

3.2.3 Characterization of ZrP nanoplates

SEM (scanning electron microscope) images before the exfoliation process were taken and shown below along with an exfoliated ZrP molecule retrieved from a TEM (transmission electron microscope) image.

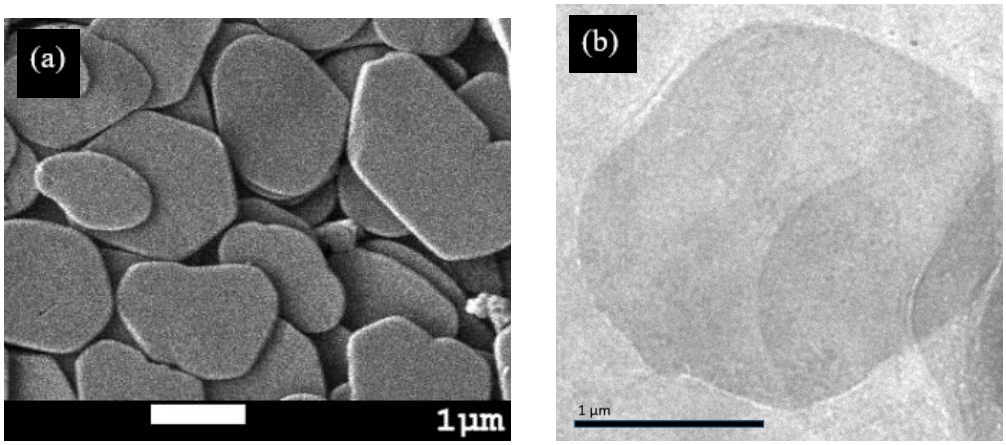

Figure 23: (a) SEM Image of ZrP molecule before exfoilation. (b) TEM image of a monolayer ZrP molecule (exfoilated with TBA)

3.2.4 Preparation of Solution in Set up Tank:

Experiments run without ZrP consisted of 400 mL of Chemguard C2 foam concentrate and 19.6 L of water. In the experiments with ZrP, 400 mL of the exfoliate d ZrP solution is added to 400 mL of Chemguard C2 foam concentrate and 19.2 L of water. The tank is mixed gently before running the experiment. The entire setup is washed by running water through it to ensure that any residual foam or particles are removed.

The set up consists of a pump that transfers liquid from the foam solution tank to the air cylinder where the liquid mixes with airflow from the fan. The foam then passes through the screen generating foam bubbles that leave the air cylinder and deposit into the foam container.

For the forced convection experiments, to achieve uni-directional flow of wind, a wind tunnel was built to reduce the turbulence effect and the figure below shows the set up. This will be used in future experiments to reduce the effect of wind turbulence. The screen mesh is made of metal and the holes are a quarter of an inch apart. The way the wind tunnel works is by the screen mesh disallowing turbulence causing only a uniform flow of wind to the other side where the foam container is located.

3.2.5 Foam height and liquid drainage measurement

Images were taken over uniform intervals of time. As the surface of the foam was not uniform in all cases, each image was analyzed using software from NIH called ImageJ which allows the estimation of average foam height for each picture.

3.3 Experimental Results

3.3.1 Expansion ratios of foam with ZrP

The expansion ratio for the foam formula with ZrP was calculated by measuring the weight of foam added in the foam container and estimating the volume of foam in the container. The average expansion ratio calculated from three trials was found to be 394 ± 40.

3.3.2 Foam height and liquid drainage with foam + ZrP

Experiments without forced convection or thermal radiation were carried out and the foam height at different time intervals was reported. The foam breakage rate for these set of experiments is shown below.

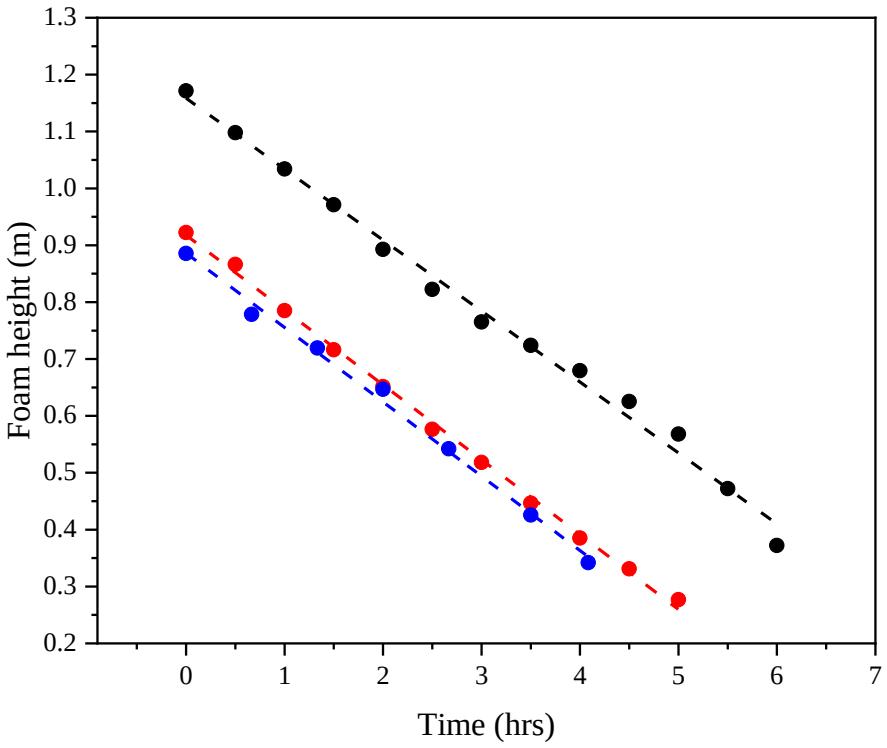

Figure 24: Foam Height vs Time without forced convection or thermal radition for the same experiment repeated three times (with ZrP-TBA)

Table 9: Foam breakage rate for the case of no forced convection or thermal radiation

Experiment	Foam breakage rate (m/hr)	(Coefficient of Determination) R^2
1	0.125 ± 0.003	0.993
2	0.132 ± 0.002	0.998
3	0.131 ± 0.004	0.995
Average	0.129 ± 0.003	

The liquid drainage for the same set of experiments showed nearly similar values and can be seen from the figure below.

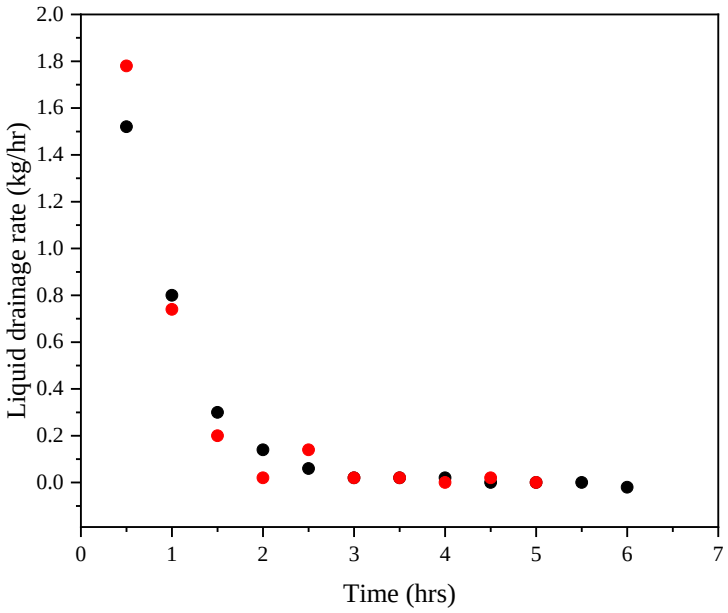

Figure 25: Liquid drainage vs Time without forced convection or thermal radition for the same experiment repeated two times (with ZrP-TBA)

Adding ZrP-TBA caused a noticeable difference in the slope where it dropped to 0.129 from 0.154 and this corresponds to a decrease in the rate of Foam breakage. This shows that ZrP can potentially help stabilize the foam and future experiments will focus on the extent of its effectiveness.

3.3.3 Foam height and liquid drainage with foam + ZrP under forced convection

The foam height at different time intervals for experiments under forced convection were carried out and a plot that yields the foam breakage rate is shown below.

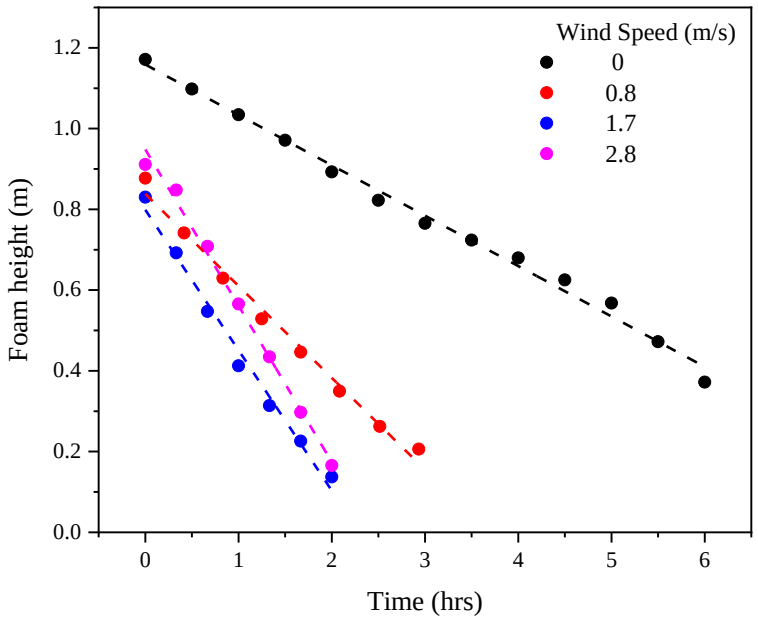

Figure 26: Foam breakage vs time with forced convection (with ZrP-TBA)

The table below shows the foam breakage rate obtained for each wind speed experiment conducted.

Table 10: Foam breakage rate (m/hr) for each wind speed

Wind speed (m/s)	Foam breakage rate (m/hr)	R^2
0	0.125 ± 0.003	0.993
0.8	0.23 ± 0.01	0.989
1.7	0.35 ± 0.02	0.988
2.8	0.39 ± 0.03	0.994

3.3.4 Foam height with foam + ZrP under thermal radiation

The figure below shows the foam height vs time for experiments performed under different intensities of thermal radiation.

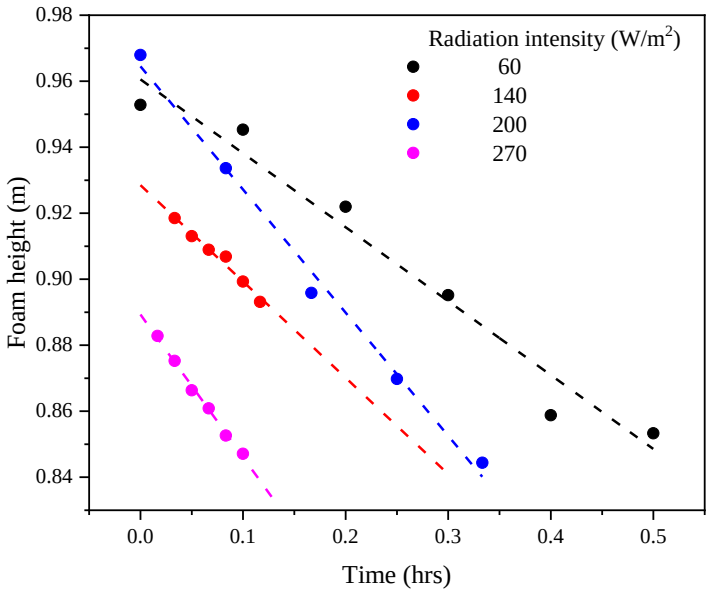

Figure 27: Foam + ZrP Height under thermal radiation

The rate is obtained by calculating the slope for each experiment and that is shown in the table below

Table 11: Foam breakage rate under different thermal radiation intensities

Radiation intensity (W/m^2)	Foam breakage rate (m/hr)	R^2
4	0.125 ± 0.003	0.993
60	0.28 ± 0.01	0.994
140	0.29 ± 0.02	0.977
200	0.31 ± 0.01	0.991
270	0.43 ± 0.01	0.995

3.4 Comparison of foam with and without ZrP

3.4.1 Comparison without the presence of LN_2

The figure below shows the foam height vs time for the experiments carried out without forced convection or thermal radiation without ZrP and another with the presence of ZrP. The two are compared through the slopes which show the foam breakage rate. The presence of ZrP has decreased the slope value of foam height vs time and this shows that ZrP has had a positive role in reducing the rate at which the foam height decreases with time.

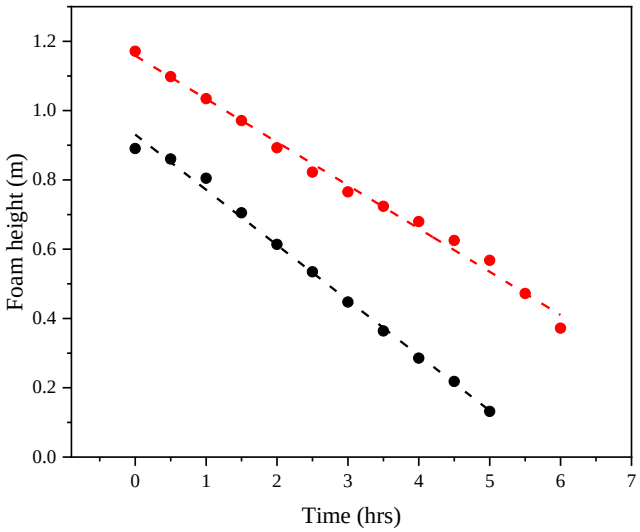

Figure 28: The stabilization of ZrP nanoplates in reducing the foam breakage rate in the case of no forced convection or thermal radiation (ZrP is red)

The corresponding foam breakage rate (slope) is shown in the table below.

Table 12: Stabilization of ZrP nanoplates in reducing the foam breakage rate in the case of no forced convection or thermal radiation.

Experiment	Foam breakage rate	R^2
Without ZrP	0.159 ± 0.004	0.995
With ZrP	0.132 ± 0.002	0.998

The liquid drainage rate was also compared and the presence of ZrP shows that initially, less liquid drains from the bubbles as compared to no ZrP molecules present. This is shown in the figure below.

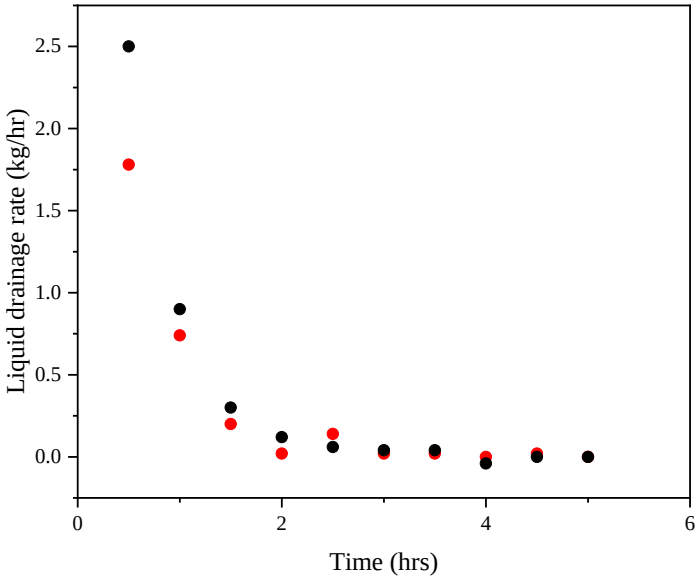

Figure 29: The presence of ZrP nanoplates in having a reduced liquid drainage rate in the case of no forced convection or thermal radiation

The figure below shows the foam height vs time for the experiments conducted under forced convection without ZrP and another with the presence of ZrP. The presence of ZrP has decreased he slope of the foam height vs time and this shows that ZrP has had a positive role in reducing the rate at which the foam height decreases with time.

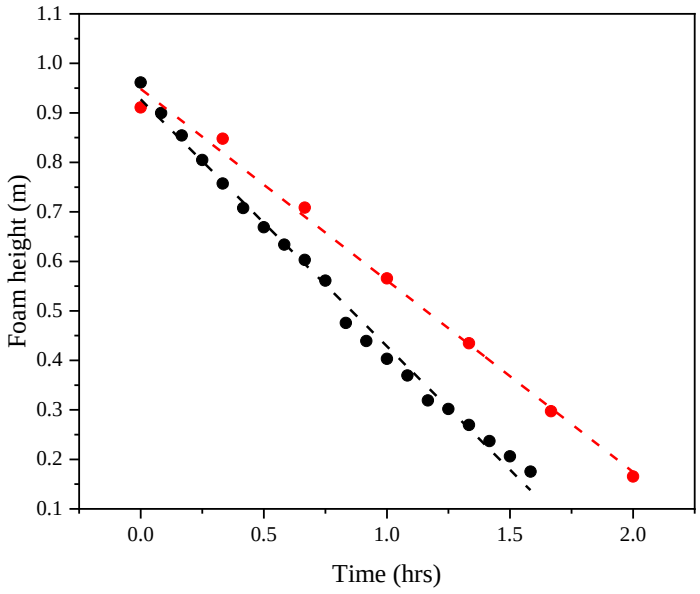

Figure 30: Foam height vs time comparison, with forced convection at highest wind speed value experimented (No ZrP = 2.5 m/s and ZrP=2.8 m/s)

The table below provides the foam breakage rate values for the comparison regarding the highest wind speed value experimented.

Table 13: ZrP nanoplates in a reduced foam breakage rate under wind induced convection

Experiment	Foam breakage rate (m/hr)	R^2
Without ZrP (2.5 m/s)	0.500 ± 0.01	0.993
With ZrP (2.8 m/s)	0.39 ± 0.03	0.994

The figure below shows the foam height vs time for the experiments conducted under forced convection without ZrP and another with the presence of ZrP. The presence of ZrP

has decreased the slope value of foam height vs time and this shows that ZrP has had a positive role in reducing the rate at which the foam height decreases with time.

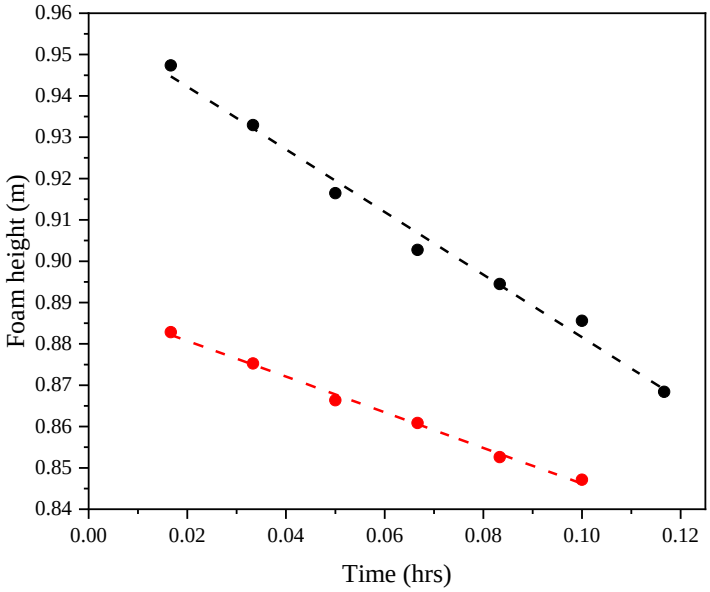

Figure 31: Foam height vs time comparison at highest thermal radiation intensity value experimented (270 W/m^2)

The table below provides the foam breakage rate values for the comparison regarding the highest thermal radiation intensity (270 W/m^2) value experimented.

Table 14: Stabilization of foam with ZrP under highest thermal radiation intensity (270 W/m2) value experimented.

Experiment	Foam breakage rate	R^2
Without ZrP	0.76 ± 0.04	0.989
With ZrP	0.43 ± 0.01	0.995

3.4.2 Comparison with the presence of LN_2

The following figure shows the foam height vs time when foam with ZrP was applied.

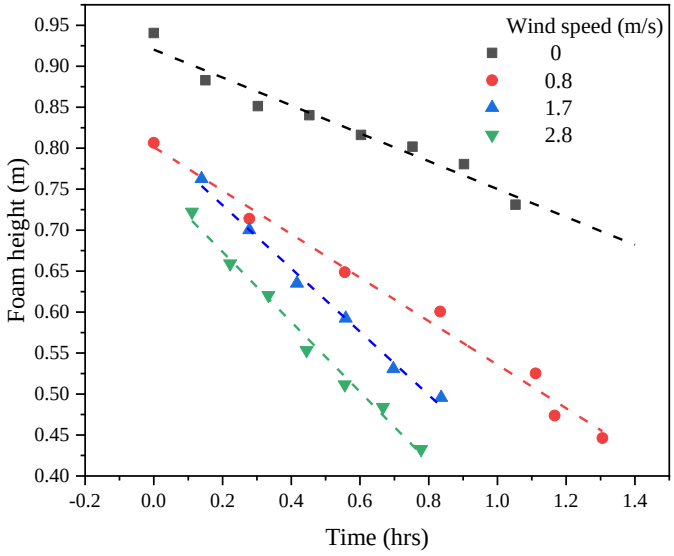

Figure 32: Foam height vs time with ZrP under different wind induced convection velocities

The following table summarizes the foam breakage rates with liquid nitrogen, with foam application with and without ZrP, under forced convection.

Table 15: Foam breakage rate comparison under the presence of wind induced convection with the presence of LN_2

Wind speed (m/s)	w/ LN_2		
	w/o ZrP	w/ ZrP	Ratio
0	0.199 ± 0.015	0.170 ± 0.015	14.573
0.8	0.350 ± 0.024	0.266 ± 0.014	24.000
1.7	0.411 ± 0.019	0.386 ± 0.017	6.083
2.8	0.513 ± 0.034	0.427 ± 0. 019	16.764

The following figure shows the foam height vs time when foam with ZrP was applied.

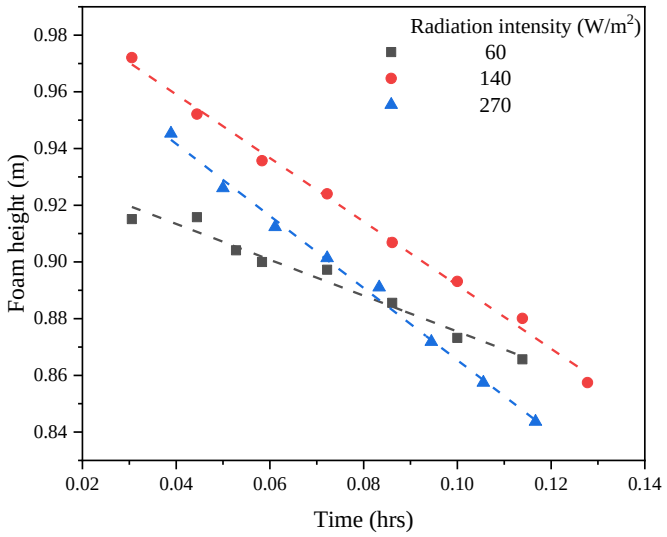

Figure 33: Foam height vs time with the presence of ZrP under different thermal radiation intensities

The following table summarizes the foam breakage rates with liquid nitrogen, with foam application with and without ZrP under thermal radiation.

Table 16: Foam breakage rate comparison under the presence of thermal radiation with the presence of LN_2

Radiation intensity (W/m^2)	w/ LN_2		
	w/o ZrP	w/ ZrP	Ratio
4	0.199 ± 0.015	0.170 ± 0.015	14.573
60	0.968 ± 0.044	0.633 ± 0.047	34.607
140	1.482 ± 0.096	1.121 ± 0.031	24.359
270	1.591 ± 0.084	1.271 ± 0.036	20.113

3.5 Discussions

The addition of exfoliated ZrP to the C2 foam formula has shown that it can enhance the stability of the foam not only by decreasing the foam breakage rate but by delaying the liquid drainage rate as well. This was true for all three cases of without forced Convection/thermal radiation, with forced convection, and with thermal radiation. Exfoilated ZrP-TBA monolayer molecule is hydrophilic on both sides allowing a strong attraction to the foam bubbles that not only would reduce surface tension between water and air due to shale antisotropy but also preventing air diffusion between the bubbles. This means that within the air interface the ZrP molecules are forming a stiff-like structure that is acting against the effect of coarsening, coalescing, and drainage of water through the bubbles; thus, slowing down these three factors It was observed that the foam breakage rate amongst different wind speeds for experiments under forced convection with and without zrp exhibited different values which are shown in the figure below. A linear fit was included.

The figure below shows the foam height comparison of adding zrp to foam under different wind speeds.

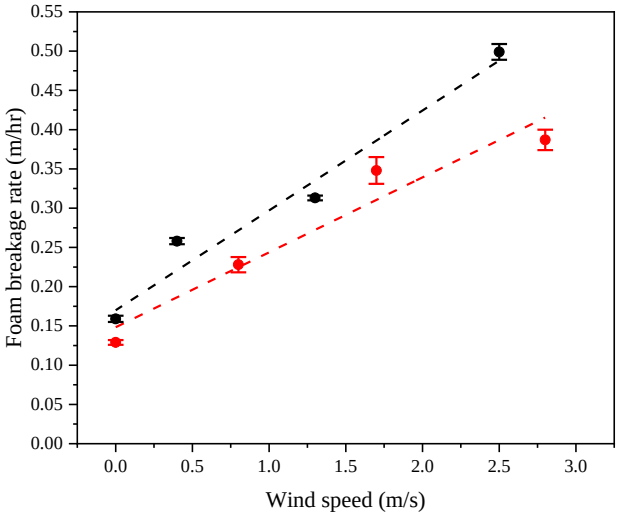

Figure 34**:** Effective resistance of ZrP stabilized foam against wind induced breakage

A comparison regarding the foam breakage rate amongst different thermal radiation intensities for the cases of with and without zrp are shown in the figure below.

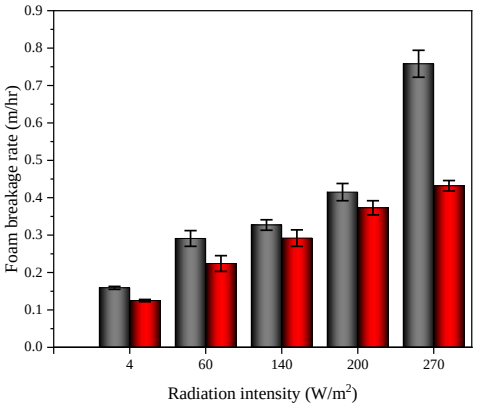

Figure 35: Foam breakage rate vs radiation intensity comparison with and without ZrP

The table below shows the comparison of the foam breakage rate when adding ZrP to foam under different radiation intensities.

Table 17: ZrP in reducing the foam breakage rate at different radiation intensities

	Foam breakage rate (m/hr)	
Radiation intensity (W/m^2)	Without ZrP	With ZrP
4	0.158 ± 0.004	0.125 ± 0.003
60	0.29 ± 0.02	0.28 ± 0.01
140	0.33 ± 0.01	0.29 ± 0.02
200	0.41 ± 0.02	0.31 ± 0.01
270	0.76 ± 0.04	0.43 ± 0.01

3.6 Conclusion

multilayer ZrP nanoparticles were exfoliated with the use of TBA and were mixed with the commercially available C2 foam formula to see its effect on stability of high expansion foam. The research result shows how ZrP was able to improve the stability of fire fighting foam by reducing the foam breakage rate and delaying the liquid drainage rate. This was the case for the experiments conducted without forced convection or thermal radiation, with forced convection, and with thermal radiation. The same trend was noticed with experiments carried out with the presence of a cryogen that exhibited similar heat transfer properties as LNG.

CHAPTER IV

CONCLUSION AND REMARKS

4.1 ZrP's effect on enhancing foam stability

High expansion foam has seen to be effective in lowering the heat transfer through convection and radiation for mitigating methane vapors in LNG and in increasing the buoyancy of the methane vapors rising upwards in the foam layers such that they travel at a level higher than groundlevel moving downwind for a better dispersion away from ignition sources. The use of exfoliated ZrP nanoparticles was shown to improve the stability of the foam allowing Exfoilating ZrP with TBA allowed ZrP to exhibit hydrophilic characteristics allowing better attraction between foam bubbles that slow down coalescining and coarsening of the foam bubbles and delay the drainage of water moving downwards by acting as a barrier to transport channels in the layers of the foam.

4.2 Future research directions

The experiments conducted in this study kept the concentration of exfoliated ZrP at a constant value of 2% of the foam solution. Other areas that may be interesting to look at are, the effect of varying the 2% volume of the ZrP nanoplates in the foam formula, using another exfoiling agent other than TBA suh as propyl amine, and further functionalizing ZrP to become more viscous or hydrophilic as shown at the Stanford Research Institute that the surface viscosity is important and may affect the stability of the foam.

BIBLIOGRAPHY

1. EIA. *Natural Gas Imports and Exports*.(2017). https://www.eia.gov/todayinenergy/detail.php?id=32912.
2. Energy information institute. International Energy Outlook 2017 Overview. 2017. https://www.energy.gov/sites/prod/files/2013/04/f0/LNG_primerupd.pdf.
3. Zhu D. Example of Simulating Analysis on LNG Leakage and Dispersion. *Procedia Eng*. 2014;71:220-229. doi:10.1016/j.proeng.2014.04.032.
4. Cabrillo. Chronological list of LNG accidents. http://citizensagainstlng.com/wp/wp-content/uploads/2014/11/Cabrillo-Port-EIR-Appendix-C3_List-of-LNG-Accidents.pdf.
5. Hamutuk L. Sunrise LNG in Timor-Leste Dreams , Realities and Challenges. 2008;(February). https://www.laohamutuk.org/Oil/LNG/LNGReportLoRes.pdf.
6. Powell T. HOW INDUSTRY AND REGULATORS KEPT PUBLIC IN THE DARK AFTER 2014 LNG EXPLOSION IN WASHINGTON Lax industry oversight and incomplete reporting leave us with What happened at Plymouth LNG ? 2016:1-8. http://www.regulatefllng.com/Mission_files/Preview of “How Industry and Regulators Kept Public in the Dark After 2014 LNG Explosion in Washington %7C Sightline Institute”.pdf.
7. Urban F, Journal L, Weinberg P. Cargo of Fire : A Call for Stricter Regulation of Liquefied Natural Gas Shipment and Storage Cargo of Fire : A Call for Stricter Regulation of Liquefied Natural Gas Shipment and Storage. 1976;4(3). https://ir.lawnet.fordham.edu/cgi/viewcontent.cgi?article=1043&context=ulj.

8. Romero S. algerian explosion stirs foes of us gas projects. *New York Times*. https://www.nytimes.com/2004/02/12/business/algerian-explosion-stirs-foes-of-us-gas-projects.html. Published 2004.

9. Schneyer J, Gardner T, Valdmanis R. Blast at US LNG site casts spotlight on natural gas safety. *Reuters*. https://www.reuters.com/article/us-lng-blast-analysis/blast-at-u-s-lng-site-casts-spotlight-on-natural-gas-safety-idUSBREA3506Y20140406. Published 2014.

10. Vanem E, Anta P, Østvik I, Del F, Comas C De. Analysing the risk of LNG carrier operations. 2008;93(March 2006):1328-1344. doi:10.1016/j.ress.2007.07.007.

11. Chemguard. Safety Data Sheet. *Wear*. 1980:4-6. doi:10.1186/1755-8166-7-33.

12. Conroy MW, Taylor JC, Farley JP, Fleming JW. Colloids and Surfaces A : Physicochemical and Engineering Aspects Liquid drainage from high-expansion (HiEx) aqueous foams during and after filling of a container. *Colloids Surfaces A Physicochem Eng Asp*. 2013;426:70-97. doi:10.1016/j.colsurfa.2013.02.050.

13. Cherifi M. Contribution to Fire Protection of the LNG Storage Tank Using Water Curtain. 2010;(December). doi:10.5383/ijtee.02.02.005.

14. Hill C, Eastoe J. Foams : From nature to industry ☆. 2017;247(March):496-513. doi:10.1016/j.cis.2017.05.013.

15. Fei Y, Jr RLJ, Gonzalez M, Haghighi M, Pokalai K. Experimental and numerical investigation into nano-stabilized foams in low permeability reservoir hydraulic fracturing applications. *Fuel*. 2018;213(November 2017):133-143.

doi:10.1016/j.fuel.2017.10.095.

16. Guevara JS, Mejia AF, Shuai M, Chang Y-W, Mannan MS, Cheng Z. Stabilization of Pickering foams by high-aspect-ratio nano-sheets. *Soft Matter*. 2013;9(4):1327-1336. doi:10.1039/C2SM27061G.
17. Chen X, Yang D, Zou Y, Yang X. Stabilization and functionalization of aqueous foams by Quillaja saponin- coated nanodroplets. *Food Res Int*. 2017;99(March):679-687. doi:10.1016/j.foodres.2017.06.045.
18. Ã BYL, Trelles J. Foam spread over a liquid pool. 2007;42:249-264. doi:10.1016/j.firesaf.2006.10.004.
19. Arzhavitina A, Steckel H. Foams for pharmaceutical and cosmetic application. *Int J Pharm*. 2010;394(1-2):1-17. doi:10.1016/j.ijpharm.2010.04.028.
20. Zhao Y, Brown MB, Jones SA. Pharmaceutical foams : are they the answer to the dilemma of topical nanoparticles ? *Nanomedicine Nanotechnology, Biol Med*. 2010;6(2):227-236. doi:10.1016/j.nano.2009.08.002.
21. Farajzadeh R, Andrianov A, Krastev R, Hirasaki GJ, Rossen WR. Foam – oil interaction in porous media : Implications for foam assisted enhanced oil recovery. *Adv Colloid Interface Sci*. 2012;183-184:1-13. doi:10.1016/j.cis.2012.07.002.
22. Zhang B, Liu Y, Olewski T, Vechot L, Mannan MS. Blanketing effect of expansion foam on liquefied natural gas (LNG) spillage pool. *J Hazard Mater*. 2014;280:380-388. doi:10.1016/j.jhazmat.2014.07.078.
23. Stevenson P, Prozorov R, Canfield PC, et al. Introduction. 2012;2000(Chapter

11):7-13.

24. Zhang L. *Masters Thesis*.; 2015.

25. Lam S, Velikov KP, Velev OD. Current Opinion in Colloid & Interface Science Pickering stabilization of foams and emulsions with particles of biological origin. *Curr Opin Colloid Interface Sci*. 2014;19(5):490-500. doi:10.1016/j.cocis.2014.07.003.

26. Kumar C V, Chaudhari A. Proteins Immobilized at the Galleries of Layered R -Zirconium Phosphate : Structure and Activity Studies. 2000;(2):830-837. doi:10.1021/ja993310u.

27. Armento P, Casciola M, Pica M, Marmottini F, Palombari R, Ziarelli F. Silica – zirconium phosphate – phosphoric acid composites : preparation , proton conductivity and use in gas sensors. 2004;166:19-25. doi:10.1016/j.ssi.2003.10.016.

28. He X, Xiao H, Choi H, et al. Colloids and Surfaces A : Physicochemical and Engineering Aspects ⎵ -Zirconium phosphate nanoplatelets as lubricant additives. *Colloids Surfaces A Physicochem Eng Asp*. 2014;452:32-38. doi:10.1016/j.colsurfa.2014.03.041.

29. Bauer F. Comparison between Nafion ® and a Nafion ® Zirconium Phosphate Nano- Composite in Fuel Cell Applications. 2006;(3):261-269. doi:10.1002/fuce.200500217.

30. Wang N. Flame Retardancy of Polymer Nanocomposites based on Layered Aluminum Phosphate and Computational Study of Intercalation of Amines into α-

Zirconium Phosphate and Adsorption of a Model Organic Pollutant. 2011.

31. Kaschak DM, Johnson SA, Hooks DE, Kim H, Ward MD, Mallouk TE. Chemistry on the Edge : A Microscopic Analysis of the Intercalation , Exfoliation , Edge Functionalization , and Monolayer Surface Tiling Reactions of R - Zirconium Phosphate. 1998:10887-10894. doi:10.1021/ja9818710.

32. Alberti GIULIO, Casciola MARIO. Inorganic Ion-Exchange Pellicles Obtained by Delamination of o ~ -Zirconium Phosphate Crystals. 1985;107(1):256-263.

33. Sun L, Boo WJ, Sun D, et al. Preparation of Exfoliated Epoxy / r -Zirconium Phosphate Nanocomposites Containing High Aspect Ratio Nanoplatelets. 2007:1749-1754. doi:10.1021/cm062993r.

34. Fang M, Kim CH, Saupe GB, et al. Layer-by-Layer Growth and Condensation Reactions of Niobate and Titanoniobate Thin Films. 1999;(7):1526-1532. doi:10.1021/cm981066k.

35. Wege HA, Kim S, Paunov VN, Zhong Q, Velev OD. Long-Term Stabilization of Foams and Emulsions with In-Situ Formed Microparticles from Hydrophobic Cellulose. 2008;282(20):9245-9253.

36. Kim H, Keller SW, Mallouk TE, Schmitt J, Sadron IC. Characterization of Zirconium Phosphate / Polycation Thin Films Grown by Sequential Adsorption Reactions. 1997;4756(97):1414-1421. doi:10.1021/cm970027q.

37. NFPA. NFPA 11: Standard for Low-, Medium, and High-Expansion Foam (2016, Current Edition). 2016. http://catalog.nfpa.org/NFPA-11-Standard-for-Low-Medium-and-High-Expansion-Foam-2016-Edition-P9074.aspx.

38. NFPA. Nfpa 16. 2007.

39. Harding B, Zhang B. Improved research-scale foam generator design and performance characterization. *J Loss Prev Process Ind*. 2016;39:173-180. doi:10.1016/j.jlp.2015.11.016.

40. Lam S, Blanco E, Smoukov SK, Velikov KP, Velev OD. Magnetically Responsive Pickering Foams. 2011:13856-13859. doi:10.1021/ja205065w.

41. Rezvantalab H, Ghazi N, Ambrusch MJ, Infante J. An Aqueous-Based Approach for Fabrication of PVDF / MWCNT Porous Composites. *Sci Rep*. 2017;(April):1-10. doi:10.1038/s41598-017-01770-9.

42. Fujii S, Iddon PD, Ryan AJ, Armes SP, Hill B, Kingdom SU. Aqueous Particulate Foams Stabilized Solely with Polymer Latex Particles. 2006;(6):7512-7520. doi:10.1021/la060812u.

43. Brown AG, C W, Thuman, McBain JW. THE SURFACE VISCOSITY OF DETERGENT SOLUTIONS AS A FACTOR IN FOAM STABILITY. 1953:491-507.

44. Liu L, Wen J, Liu L, He D, Kuang R, Shi T. A mediator-free glucose biosensor based on glucose oxidase / chitosan / a -zirconium phosphate ternary biocomposite. *Anal Biochem*. 2014;445:24-29. doi:10.1016/j.ab.2013.10.005.

45. Xia F, Yong H, Han X, Sun D. Small Molecule-Assisted Exfoliation of Layered Zirconium Phosphate Nanoplatelets by Ionic Liquids. *Nanoscale Res Lett*. 2016:0-6. doi:10.1186/s11671-016-1559-6.

46. Takeno K, Ichinose T, Tokuda K, Ohba R, Yoshida K, Ogura K. Effects of high

expansion foam dispersed onto leaked LNG on the atmospheric diffusion of vaporized gas. *J Loss Prev Process Ind*. 1996;9(2):125-133. doi:10.1016/0950-4230(95)00062-3.

47. Carrier V, Colin A. Coalescence in Draining Foams. 2003:4535-4538.

48. Li X, Karakashev SI, Evans GM, Stevenson P. Effect of Environmental Humidity on Static Foam Stability. 2012. doi:10.1021/la205101d.

49. Zhang BIN. Ph.D Dissertation. 2015;(December).

50. Mejia AF, Chang Y, Ng R, Shuai M, Mannan MS, Cheng Z. Aspect ratio and polydispersity dependence of isotropic-nematic transition in discotic suspensions. 2012;61708:1-12. doi:10.1103/PhysRevE.85.061708.